HHS Public Access

Author manuscript

Nanoscale. Author manuscript; available in PMC 2021 May 11.

Published in final edited form as:

Nanoscale. 2019 January 17; 11(3): 799–819. doi:10.1039/c8nr07769j.

Applications of Nanoparticles in Biomedical Imaging

Xiangjun Han[a], **Ke Xu**[a], **Olena Taratula**[b], **Khashayar Farsad**[c]

[a.]Department of Radiology, First Hospital of China Medical University, Shenyang, Liaoning,110001 P. R. China.

[b.]Department of Pharmaceutical Sciences, College of Pharmacy, Oregon state University, Corvallis, Oregon 97331, USA

[c.]Charles T. Dotter Department of interventional Radiology, Oregon Health and Science University, Portland, Oregon 97239-3011, USA

Abstract

An urgent need for early detection and diagnosis of diseases continuously pushes the advancements of imaging modalities and contrast agents. Current challenges remain for fast and detailed imaging of tissue microstructures and lesion characterization that could be achieved via development of nontoxic contrast agents with longer circulation time. Nanoparticle technology offers this possibility. Here, we review nanoparticle-based contrast agents employed in most common biomedical imaging modalities, including fluorescence imaging, MRI, CT, US, PET and SPECT, addressing their structure related features, advantages and limitations. Furthermore, their applications in each imaging modality are also reviewed using commonly studied examples. Future research will investigate multifunctional nanoplatforms to address safety, efficacy and theranostic capabilities. Nanoparticles as imaging contrast agents have promise to greatly benefit clinical practice.

1. Introduction

Early detection and diagnosis of disease is a crucial part of clinical practice, especially for cancer. For example, the two-year survival rate of gastrointestinal cancer patients for those who benefited from early detection has been observed to be much higher than in those without early detection (92.3% VS 33.3%).[1] In addition, the ten-year mortality rate for breast cancer patients who benefited from early detection was reduced by 17–28%.[2] Medical imaging technology often plays the most important role in the early detection and therapeutic response assessment of various diseases. Imaging modalities in current use include X-ray radiography, computed tomography (CT), magnetic resonance imaging (MRI), ultrasound (US), positron emission tomography (PET), single photon emission computed tomography (SPECT), and fluorescence imaging (Fig. 1).[3] To improve lesion detection, very often more than one imaging modality is combined.[4, 5] To get more accurate

Kxu@cmu.edu.cn.

Conflicts of interest

There are no conflicts to declare.

anatomic and functional information, medical imaging contrast agents are used to distinguish between normal tissue and abnormal lesions. For traditional clinical imaging contrast agents, tumor detection is limited by the spatial resolution generated by the imaging hardware, such as the ability of contrast-enhanced CT to detect a hypervascular hepatoma as small as 3 mm.[6] Currently used medical imaging contrast agents are mostly small molecules that exhibit fast metabolism, and have non-specific distribution and potential undesirable toxicities.[7, 8]

Recently, nanomaterials have stimulated efforts in improving biomedical detection and imaging due to unique passive, active and physical targeting properties. Due to their small size, nanoparticles exhibit enhanced permeability and retention (EPR) effects in tumors, with relative increases in local tumor concentrations of contrast agent.[9] Among all features of the nanoparticle, size plays a particularly important role for tumor imaging. Nanoparticle size significantly influences biodistribution, blood circulation half-life, cellular uptake, tumor penetration and targeting.[10] As the average renal filtration pore is 10 nm,[11] nanoparticles with sizes less than 10 nm are rapidly cleared by the renal excretion system.[12] By contrast, nanoparticles with sizes over than 100 nm are easily identified by macrophages and accumulate in organs with the mononuclear phagocyte system (MPS), such as lymph nodes, liver, spleen and lung.[13] Furthermore, several reviews summarized that nanoparticle sizes between 10 to 60 nm have consistently demonstrated enhanced cellular uptake.[10, 14]

In addition to passive targeting strategies, nanoparticle surface labeling with various ligands to target receptors can increase imaging contrast agent localization through specific binding to target receptors in lesions.[15–17] For example, gold nanoparticles surface decorated with a prostate-specific membrane antigen RNA aptamer have been shown a higher CT density for prostate cancer cell imaging.[18] In addition, nano-sized superparamagnetic iron oxide (SPIO) agents surface decorated with a high-affinity anti-EGFR antibody have been shown to target lung tumors by MRI.[19]

Antibodies and antibody fragments are the most common and efficient active targeting ligands. Antibodies have a high specific affinity to the corresponding antigens which can increase nanoparticle concentration to a specific location.[20] Another ligand used for targeting is an aptamer, which is also named as a chemical antibody. It is a single DNA or RNA sequence that folds into a secondary structure with a high targeting affinity to cell surface receptors. Compared with antibodies, aptamers are small, easy to synthesize and confer lower immunogenicity.[21] However, aptamers are rapidly cleared by the renal system and degraded by nucleases, preventing the desired blood circulation time for effective tumor localization.[22, 23] Peptides represent an additional ligand targeting moiety, with benefits including chemical stability, ease of synthesis and reduced immunogenicity.[24] The arginine-glycine-aspartic acid (RGD) peptide is the principal integrin-binding doman and can bind to multiple integrin species,[25] it is very common in nanoparticle application.[26] Other proteins and molecules with active targeting roles include transferrin, folic acid and biotin.[27]

In addition to active and passive targeting strategies, various stimuli also play a targeting role in nanoparticle imaging applications, In these physical targeting strategies, external sources or fields guide nanoparticles to the target site and control the release process, as seen

in photothermal and magnetic hyperthermia therapy.[28] An acidic pH/reduction dual-stimuli responsive nanoprobe for enhanced CT imaging of tumor is another example.[29] For all targeting types, drug release can be triggered by a change in pH, temperature, or a combination of both. The pH, temperature, enzyme activity and redox gradient belong to endogenous stimuli, and light, magnetic and ultrasound belong to external stimuli.[30]

Compared to traditional contrast agents, prolonged blood circulation time of nanoparticle-based contrast agents plays a key role for their enhanced contrast signal. Nanoparticle modification to promote circulation time is thus a critical factor in imaging performance. The most common modification method is encapsulation of hydrophobic nanomaterials in a polyethylene glycol (PEG) shell,[31] which greatly increases solubility and prolongs blood circulation time. Due to the hydrophilic backbone of PEG, nanoparticle binding to opsonins and recognition by macrophages is decreased, reducing nanoparticle clearance by the reticuloendothelial system (RES).[32, 33] Dextrose and polysaccharide, such as chitosan, hyaluronic acid and fucoidan, play a similar role in prolonging nanoparticle circulation.[34, 35] Zwitterionic modification endows nanoparticles with surface properties resistant to aggregation, binding plasma proteins and macrophage uptake, significantly prolonging circulation time.[36, 37] Additionally, albumin surface modification of nanoparticles increases blood circulation time while maintaining biological activity and decreasing immunogenicity.[38]

Due to improved targeting strategies and a long circulation life in blood, nanoparticles have been studied for early tumor detection and diagnosis.[39] Nanoparticles have been used for early detection in three major ways. The most common use has been employing nano-contrast agents with existing imaging modalities. For instance, gold nanocages conjugated with α-melanocyte-stimulating hormone (α-MSH) peptide and ^{64}Cu radiolabeled melanocortin 1 receptor-(MC1R) have been used for melanoma detection by PET in a mouse model.[40] Nanoparticles can also act as specific delivery platforms loaded with other imaging elements to identify cancers. An example includes the liposome encapsulated gold nanoclusters functionalized with Her2 antibody to detect human breast cancer cells in serum and tissue by colorimetry.[41] Additionally, nanoparticles can be employed for selective tumor biomarker detection.[42, 43] Early detection of certain cancer biomarkers can be very challenging, and nanoparticles have been used to magnify the signal. For example, a nano-genosensor was found to significantly amplify the signal from the known breast cancer biomarker, miRNA-21, in clinical samples.[44] Nano-immunosensor was employed to ultrasensitively detect cancer antigen 15–3 for breast cancer in human plasma samples.[45] Other uses of nanoparticle detection have included identification of circulating tumor cells (CTCs).[46]

In contrast to traditional contrast agents, nano-imaging agents demonstrate a high surface area to volume ratio enabling surface labeling with specific molecules and ligands to improve the toxicity profile and imaging properties.[47, 48] Additional benefits of imaging nanoparticle include functional visualization and monitoring of biological processes, such as macrophage detection in atherosclerotic lesions using CT,[49] and molecular imaging of angiogenesis by MRI.[50] Furthermore, the prolonged plasma circulation time of nanoparticles improves biodistribution with a greater lesion to background contrast signal.[51] Additionally,

the shape and size of the nanoparticles can be manipulated to optimize the loading of imaging compounds, and their intrinsic physical properties can also be changed to meet specific clinical needs.[52, 53]

Considering the limits of current imaging contrast agents and the potential advantages of nanoparticles for early diagnosis and microstructure visualization, interest in nanotechnology for biomedical imaging is rapidly increasing. A search for the term “nanoparticle and imaging” on PubMed shows a significant recent increase in the number of relevant publications, highlighting the intense efforts being placed in this domain (Fig. 2). Synthesis and decoration of nanoparticles, with features related to therapeutic use, pharmacokinetics and toxicity have been reported.[54, 55] In this review, we summarize the application of nanoparticles with different imaging modalities, including fluorescence imaging, MRI, CT, US, PET, and SPECT. We mainly focus on structural properties of nanoparticles and pertinent biomedical imaging applications, including for cancer imaging and other diseases. Commonly studied examples for each imaging modality are discussed.

2. Nanoparticles in fluorescence imaging applications

2.1 Advantages and limits of fluorescence imaging

Although MRI, CT, US, SPECT and PET are commonly used to detect lesions, imaging resolution remains on a macroscopic level.[6, 56] Fluorescence imaging technology can provide the highest spatial resolution for disease diagnosis on a microscopic level, especially with near-infrared fluorescence (NIRF) imaging. Compared with visible light, NIRF has advantages of deeper tissue penetration and less non-specific tissue auto-fluorescence. Despite this, the penetration depth remains limited, and auto-fluorescence and scattering properties in various tissues continues to hinder clinical utility.[57] Furthermore, limited fluorescence in the target lesion and potential blink and photobleaching effects can lead to low sensitivity for detecting abnormalities.[57, 58]

Nanoparticles have useful properties to overcome the potential limitations of fluorescence imaging. For instance, a greater number of fluorescent dye molecules can be loaded in nanoparticles to provide more signals.[59] In addition, the nanoparticles can be modified (or structured) in order to prevent the potential quenching of NIR fluorescence when needed.[60] Furthermore, both active and passive strategies can be utilized to increase nanoparticle concentrations in lesions, and then increase the local lesion concentration of fluorescent dye. Additionally, the relatively long time in circulation facilitates greater uptake in target lesions. Nanoparticles can also be designed to convert lower energy photons to higher energy photons, which is important to reduce the blink and photobleaching effects.[61] As a result of these useful properties, extensive effort has been placed on the development of fluorescent nanoparticle platforms (Fig. 2).

2.2 Structure and composition features

The commonly used nanoparticle designs for fluorescence imaging in preclinical research are shown in Fig. 3. The first and most common design incorporates surface-labeled fluorophores as vectors (Fig. 3A). One of the examples is a plasmonic/magnetic nanoparticle

conjugated with the Cy3- modified S6 aptamer.[62] where the fluorescent dye provides imaging while nanoparticles enable higher local concentrations via passive and active targeting. Another design, known as a “core-shell” structure (Fig. 3B), uses a fluorescent dye that is loaded into the center of nanoparticles, with the nanoparticle’s outer shell labeled with antibodies, ligands, and peptides. Examples of core-shell designs include micelles[63], dendrimer[64,] and Qdot quantum nanoparticles,[65] and multi-layered nanomatryoshka[66] (Fig. 4). Advantages of these designs include solubilizing hydrophobic fluorophores and protecting inner fluorophores from rapid degradation and excretion.,

A third design uses concentrated fluorescent dye quenched within nanoparticles (Fig. 3C) to improve the resolution and target-to-background ratio, with potentially greater sensitivity with imaging. In this design, the nanoparticle absorbs energy from fluorescent dyes as a quencher that keeps the signal in an “off” state while in circulation. When the nanoparticles concentrate at the target site, the nanoparticle is being degraded by molecules such as caspase, protease, and DNase, releasing the dye from the nanoparticle and alleviating the quenched state. The fluorescence of the dye thus turns to an “on” state. This design platform has been leveraged to detect protease activity, apoptosis, tumor, and inflammation.[67–69] The fourth design is similar to the previous (Fig. 3D), only the fluorescent dye is combined with a separate quenching molecule, and then the combination is incorporated into nanoparticles. Proteases or other cleaving enzymes, including DNAzymes (Zn-Enz)/AuNP-FAM/BHQ-1 or streptavidin modified CdSe/ZnS quantum dots connected with biotin-peptide-BHQ-1, play a key role in activating the nanoplatform and providing localized NIR fluorescence.[70, 71]

In addition, there is one more design for nanoparticle-based fluorescence imaging using Forster resonance energy transfer (FRET) (Fig. 3E). FRET is a process whereby energy is transferred from a donor molecule to an acceptor molecule, with the energy released creating fluorescence.[72] There are two kinds of energy transferred modalities.[73] The first is the Stokes shift, which involves photon energy changes from high to low producing longer wavelength light.[74] The second involves nanoparticle production of high energy, visible wavelength photons upon absorption of lower energy NIR light, termed the anti-Stokes shift. The upconversion nanoparticle (UCNP) uses this mechanism.[75] Since ultraviolet and visible light have more energy and shorter wavelengths than NIR light with longer wavelengths, NIR becomes a better excitation light source in order to both decrease potential tissue damage from high photon energy and increase tissue penetration depth to improve the signal-to-background ratio. There is a spectral range from 650 to 1300 nm where biological tissue has minimal absorption and scattering, and autofluorescence of tissue is minimal. UCNPs can therefore effectively convert NIR excitation (650–950 nm) to significant fluorescence for imaging.[61, 76]

2.3 Application in biomedical imaging

Nanoparticle fluorescence imaging has been used in gene detection, protein analysis, enzyme activity evaluation, element tracing, cell tracking, early stage disease diagnosis, tumor related research, and monitoring real time therapeutic effects.[59, 67, 77–81] Examples from the literature are summarized in Table 1, including nanoparticle composition, imaging

agent, nanoparticle size, biomedical applications, and whether the concept has been shown in vivo or in vitro.

2.4 Examples used in fluorescence imaging

Quantum dots (QDs) are semiconductor crystals with a typical core-shell structure, the sizes of which are between 1 to 10 nanometers.[3, 82] There is an energy distance between the valence and conduction layers which is termed the band gap. Different sizes of quantum dots determine different band gaps, and different band gaps need different energies to excite the quantum dots.[83] Quantum dots, therefore, have broad absorption spectra and tunable fluorescence emission. Quantum dots operate via FRET, with a large Stokes shift producing long wavelengths to increase tissue penetration depth and reduce background autofluorescence.[84, 85] Quantum dots are photostable with a narrow and symmetric emission band, have an excellent molar extinction coefficient that is more than 10 times larger than that of organic dyes, are relatively long-lived to create a better signal to noise ratio, and therefore typically demonstrate a very bright light.[65]

However, some negative properties of quantum dots should be adressed.[56] The first is element composition. The cadmium, lead, mercury, arsenic ion released from quantum dots may have cytotoxic effects.[73, 86] The second is the fact that quantum dots are hydrophobic and require solubilization via hydrophilic shells that must not hamper the energy transfer process. These shells, however, can be labeled with various ligands, peptides, and antibodies, and thus quantum dots have been used in molecular imaging, gene and protein identification, cellular tracking, virus detection, cancer diagnosis, and drug monitoring and delivery applications.[85, 87–90]

Nanoparticles with quenching effects are important for fluorescence imaging when there is interest to control the fluorescence between an “on” and “off” state. Gold nanoparticles (AuNP) ranging in size from single digits to hundreds of nanometers have high fluorescence quenching efficiency and thus have been used for this purpose.[91–93] AuNPs also have other beneficial properties including photostability, biocompatibility, variable sizes, strong light scattering in dark field microscopy and ease of surface labelling.[94] Graphene oxide also exhibits excellent quenching effects with relatively low cost and high sensitivity. Also, graphene has good solubility and stability in water and various solvents. The main functional group is peripheral carbon sheets. Graphene nanoparticles have been mainly used in gene and protein detection.[95, 96] Carbon nanotubes have a similar mechanism and function as graphene.[97, 98] Dark quenchers are a group of molecules with quenching effects, but with no nanoparticle structure and no fluorescence. They are used in conjunction with nanoparticles and fluorophores. Commercially available dark quenchers include Dabsyl, Black Hole Quenchers (BHQ), Qxl quenchers, Iowa black FQ, Iowa black RQ and IRDye QC-1. In biomedical applications, dark quencher nanoparticles and molecules have been widely used in gene and protein detection, tumor early detection, and ion tracing, especially for enzyme activity evaluation, such as matrix metalloproteinase and caspase.[68, 70, 99, 100]

Upconversion nanoparticles (UCNPs) play a key role in fluorescence imaging. Lanthanides are essential for up conversion nanoparticles, also termed rare earth doped up conversion nanoparticles.[72] The rare earth series consists of 17 elements, with only Scandium (Sc) and

Yttrium (Y) being non-lanthanide rare earth elements. The typical element in common clinical applications is gadolinium (Gd), used for MRI contrast. UCNPs are co-doped nanoparticles which include an absorber and an emitter. Absorber elements usually consist of La, Nb, Gd, Y, Yb ions, while emitter elements are Tm, Er, Yb, or Ho.[61, 105, 106] The size of UCNPs usually ranges from 8 to 550 nm,[105, 107] and they can absorb NIR light and emit higher energy light from ultraviolet to far red light.[75, 108] UCNPs are photostable, biocompatible, and have bright fluorescence. In earlier examples, their hydrophobic property requires solubilizing with hydrophilic surface molecules with attached fluorescent dyes to image. UCNPs have been used in protein detection, cell imaging, and cancer diagnosis.[61, 109, 110]

3 Nanoparticles in MRI imaging applications

3.1 Advantages and limits of MRI

MRI is a powerful imaging modality which has long been in clinical use. It is based on proton spin in the presence of an external magnetic field when excited with a radio frequency pulse. Depending on the nuclear magnetic resonance signal from protons in human bodies, MRI provides high spatial resolution, temporal resolution, and excellent intrinsic soft-tissue contrast. It also has the ability of showing anatomic tomographic information in the three-dimensional form. Moreover, MRI uses non-ionizing radiation or radiotracers. Limitations of MRI include cost, longer imaging times, motion artifact and potential foreign body/implant artifacts. MRI contrast agents significantly help lesion detection and differentiation from healthy tissues.[111, 112]

3.2 Structure and composition features

Hydrogen protons play a key role in the mechanism of MRI, as all protons align their spin in one direction under the control of an external magnetic field. After application of a radiofrequency pulse, the proton spin orientation is deflected and then subsequently relaxes to the original state. This process generates two independent relaxation parameters known as the T1 and T2 relaxation times. MRI contrast agents can be divided into three categories. The first is T1-weighted contrast agents. Most MRI contrast agents used in modern medicine belong to this category, including gadolinium (Gd^{3+}) chelated materials.[113] T1 imaging agents are typically paramagnetic materials that shorten the T1 relaxation time resulting in bright contrast on T1-weighted images. This category of contrast agent represents the ‘positive’ contrasts. The second category is T2-weighted contrast agents. T2 imaging agents are typically superparamagnetic materials that shorten T2 relaxation times, leading to dark contrast on T2-weighted images. This category represents the ‘negative’ contrasts. Superparamagnetic iron oxide (SPIO) is a commonly used agent in this category,[114] the main component of which is magnetite (Fe_3O_4) or maghemite (Fe_2O_3).[115] The last category is dual-weighted contrast agents enabling both T1-weighted and T2-weighted contrast. An example includes gadolinium oxide nanoparticles (Gd_2O_3).[116] Due to abundant water and carbohydrate in living tissues, the traditional hydrogen MRI (^{1}H-MRI) usually has high background signals. Heteronuclear MRI atoms, including ^{13}C, ^{23}Na, ^{17}O, ^{31}P, ^{15}N and ^{19}F, have been developed to address this limitation.[117–121] These elements are in natural abundance and can be detected by MRI, generating high contrast–to–noise ratios. ^{19}F

fluorinated perfluorocarbons, in particular, have attracted much attention as cell tracking, tumor labeling, and lung imaging agents[122]

The common structural designs amongst MRI contrast agents in nanosized particles are illustrated below. The most standard design is a magnetic nanoparticle with surface decoration. This is a basic structure, which can be employed directly or as the original magnetic materials to develop new nanoparticles (Fig. 5A). Superparamagnetic iron oxide nanoparticle (SPIO) is an example of this design.[123] Another design is a core-shell structure, with magnetic materials synthesized as the core with organic or inorganic materials used for the shell (Fig. 5B). Examples of this structure include micelles and dendrimers.[114, 116] The core-shell design enables some control of nanoparticle size and the amount of loaded magnetic materials. Furthermore, this design also has advantages of improved solubility and biosafety. As shown in Fig. 4, the shell can decrease the release of metal ion and also greatly increase the relaxivity. A third design uses a vector structure, with magnetic materials used in surface adhesion or ligand connection to other nanoparticles (Fig. 5C). The surface modification provide MRI contrast, and the main nanoparticle can have other functions such as fluorescence imaging, CT imaging and drug loading properties.[124, 125] Other designs use a mixed structure, with magnetic materials loaded in both the center and surface of nanoparticles to provide increased contrast. An example includes liposomal-gadolinium (Fig. 5D).[126] Nanoparticles used in heteronuclear MRI are usually synthesized by polymer and (or) lipid, and the heteronuclear MRI atoms are embedded in the polymer and lipid. Due to their hydrophobic properties, these agents commonly form nano-emulsions with self-assembly in aqueous environments.[117, 127]

3.3 Application in biomedical imaging

The nanometer scale of these novel contrast agents can enable MRI imaging to be used at the gene, protein, cell and organ levels.[123, 128] The nanoparticle targeting strategy is an important consideration for image optimization. For active targeting, surface labelling plays a key role in the biodistribution of nanoparticles. Specific antibodies, ligands and peptides as surface labels, for example, have been used for tumor diagnosis.[114] For passive targeting, the size of the nanoparticle is the most important feature, which can range from several nanometers to hundreds of nanometers. This strategy has been used in tumor imaging through the EPR effect. Other applications rely on non-specific cellular uptake, such as blood pool contrast imaging, inflammation imaging, malignant lymph node identification, mesenchymal stem cell tracking and islet transplantation monitoring. Examples of MRI contrast nanoparticles from the literature are summarized in Table 2, including, nanoparticle composition, imaging methods, nanoparticle size, biomedical applications, and whether the concept has been shown in vivo or in vitro.

3.4 Examples used in MRI imaging

Gadolinium belongs to the rare earth element group, with its paramagnetic property reducing the longitudinal relaxation time (T1) to create bright images on T1 weighted imaging. Gadolinium is currently the most common ‘positive’ MRI contrast agent. Due to toxicity of free gadolinium ions, clinical contrast agents are in the form of gadolinium chelates, or otherwise need surface conjugation. Currently, the clinically approved MRI contrast agents

are mainly based on gadolinium (Gd Ⅲ) complexes. With the development of nanotechnology, gadolinium has been incorporated into nanosized contrast agents to play more powerful roles. For example, the nanoparticle made from high-density lipoprotein (HDL) conjugated with Gd^{3+} chelates can localize atherosclerotic plaque in the arterial wall.[129] In addition, the Gd^{3+} enriched DNA-AuNP has been used in genetic MRI imaging after endocytosis.[125]

Ferric oxide based MRI contrast agents have the property of reducing T2 relaxation time to produce dark images on T2 weighted imaging to create 'negative' MRI contrast. Three types of iron-based nanoparticles are currently used in biomedical imaging applications. The first group is SPIO, which represents the greatest focus of research effort. The size of SPIO nanoparticles ranges from several to thousands of nanometers. Based on their overall diameter (hydrodynamic diameter), they are classified into large SPIO (LSPIO) nanoparticles at 300–35,000 nm; standard SPIO (SSPIO) nanoparticles at 60–150 nm; ultra-small SPIO (USPIO) nanoparticles at 10–40 nm; and monocrystalline iron oxide nanoparticles at 10–30 nm, which is a subset of USPIO.[115] The second group is the magnetic iron oxide nanoparticle (MION). When larger than 10 nm, MION can be used as a negative contrast agent, while if smaller than 5 nm, named extremely small MION (ES-MION), it has the potential of being a positive contrast agent.[143] The third group is cross linked iron oxide, made from monocrystalline iron oxide with cross linked dextran coating.[144] Ferric oxide MRI contrast agents have been used in various biomedical imaging applications, such as molecular imaging, gene monitoring, cell tracking, blood pool imaging, lymph node identification and cancer diagnosis.[123, 130, 131, 145, 146]

Besides Gd^{3+} and ferric iron based MRI contrast agents, there are other nanoparticles with MRI contrast. For example, manganese based MRI contrast agents have a T1 shortening function. Manganese typically exists as Mn^{2+} in MRI contrast nanoparticles, and also can take the form of nanocrystals combined with other metal elements.[147, 148] Manganese based nanoparticles have been used in cancer diagnosis, apoptosis identification, and lymph node differentiation.[132, 133, 148] Recently, fluorinated graphene oxide (FGO) and superparamagnetic iron platinum nanoparticles have also been explored as MRI contrast agents,[149–151] but the work is still preliminary.

As discussed above, ^{19}F-MRI nanoparticles have been developed from highly fluorinated compounds, including perfluorinated crown ethers and perfluorocarbons.[152, 153] These agents have been used in cancer detection,[142] enzyme activity evaluation,[154] cell imaging and lymph node detection,[153] and drug delivery tracking.[155]

4 Nanoparticles in CT imaging applications

4.1 Advantages and limits of CT

Computed tomography (CT) takes advantage of differential tissue X-ray attenuation and thickness to create cross-sectional and three-dimensional images. As a result of faster examination speed, decreased cost, improved efficiency, and higher spatial resolution for clinical imaging, CT has quickly supplanted plain-film radiography despite the greater amounts of ionizing radiation exposure. CT contrast agents play a crucial role in

distinguishing amongst tissues with similar attenuation coefficients. Currently, intravenous CT contrast agents are mainly based on iodine. Limitations of iodinated contrast agents include fast clearance, potential renal toxicity, nonspecific blood pool distribution and documented adverse events/anaphylaxis. As a result, nanosized contrast agents have been introduced to overcome these limitations and increase the scope of CT imaging.

4.2 Structure and composition features

There are two categories of CT contrast agents based on nanoparticle composition. The first includes iodine based contrast agents, in part because of its long track record in clinical imaging. Nanoparticles are used as vectors to load iodine using the classical core-shell structure (Fig. 5B). Iodine is loaded in the nanoparticle core, as in liposomal iodine.[156] The second category is metal based contrast agents, whereby nanoparticles are made using various metals with high X-ray attenuation coefficients. Metals used in this category include gold, tantalum oxide, and zirconium dioxide.[157, 164, 165] These metal-based nanoparticle structures are similar to those for MRI imaging nanoparticles, such as basic, core-shell and vector platforms. For basic structure (Fig. 5A), gold nanoparticles are the most common example, used in translational research as a CT imaging contrast agent.[159, 166] For core-shell designs, metal elements can be incorporated either in the core or in the shell. Examples include nanoparticles with a core of gold nanospheres coated with indocyanine-loaded mesoporous silica shells (Fig. 5B),[167] and nanoparticles incorporating zirconium dioxide in the shell with PPy and doxorubicin in the core (Fig. 5E).[168] For vector designs, the metal elements act as surface materials, such as seen in poly(acrylic acid)bridged gadolinium nanoparticles with surface gold elements (Fig. 5C).[169]

4.3 Application in biomedical imaging

Nanosized CT contrast agents have been used in multiple roles based their cellular uptake, ability to generate robust CT attenuation, and their targeting capabilities. For example, gold nanoparticles engulfed by red blood cells have been used to image blood flow.[158] Liposomal iodine with a long circulation time and strong CT enhancement has been used to evaluate tumor vessels.[156] Prostate specific membrane antigen combined with aptamer in gold nanoparticles has been used to image prostate cancer.[18] Finally, zirconium dioxide nanoparticle accumulation has been used to image tumor and monitor drug distribution.[168, 170] Examples of CT nano-imaging agents in the literature are summarized in Table 3, including nanoparticle composition, size, biomedical applications, and whether the concept has been shown in vivo or in vitro.

4.4 Examples used in CT imaging

Gold nanoparticles (AuNP) have been used in various biomedical imaging applications. As a result of high atomic number, the X-ray absorption efficiency of gold is greater than that of iodine based agents, bones, and soft tissues (5.16 vs 1.94, 0.186 and 0.169 cm2/g at 100keV respectively).[171] Gold has a high biosafety profile and is easily made into various sizes and shapes. Compared with iodine based contrast agents, AuNP has no potential for renal injury or osmotic damage, and the high x-ray coefficient attenuation improves contrast resolution.[172] The diameter of AuNP ranges from several to hundreds of nanometers, but sizes in the range from 4 to 30 nm have maximal stability and cell specificity.[52] AuNP can provide

stable X-ray attenuation without considering changes caused by different shapes and sizes.[52] AuNP can act as a tracer by cellular uptake, and has been used to label tumor cells to monitor tumor growth under X-ray,[159] and to label red blood cells to image flow.[158] Other working mechanisms include active and passive targeted accumulation (Fig. 6),[173] such as in tumors to both identify cancer and facilitate radiotherapy.[160]

Iodine based liposomal nanotechnology has been used in order to minimize risks of iodinated contrast. Liposomes use a lipid bilayer on the nanometer scale, have been long applied in biomedicine as a vector, and were introduced as CT contrast agents three decades ago.[174, 175] Liposomal iodine contrast agents can be made from 100 to 400 nanometers in size.[53, 156] Compared with conventional iodine based contrast, liposomal iodine nanoparticles have lower osmotic pressure, longer blood circulation time and more powerful enhancement.[156] Liposomal nanoparticles can be used as target lesion imaging contrast agents based on cellular uptake, specific surface binding, or via the EPR effect.[53, 176]

5 Nanoparticles in ultrasound imaging applications

5.1 Advantages and limits of ultrasound

Ultrasound (US) imaging is one of the most widely used medical diagnostic imaging modalities due to its portability, noninvasiveness, high spatial resolution, low cost and real-time imaging properties. Ultrasound contrast agents have been developed to enhance the acoustic signal differences between normal tissues and target lesions. Current commercially available ultrasound contrast agents comprise of microbubbles ranging in scale from 1 to 8 um.[177] These relatively large particles only provide blood pool contrast signals rather than cellular uptake, and due to the larger size, have a relatively short circulation life time and low stability.[178] Nanotechnology has been explored to overcome these limitations; however, in order to get enough acoustic reflection, US contrast nanoparticles typically need to be larger than CT or MRI contrast nanoparticles, ranging from hundreds to thousands of nanometers. [179, 180]

5.2 Structure and composition features

The size of most US contrast nanoparticles is about 200 nanometers.[177, 181] These nanoparticles can be readily labeled with various surface ligands for specific binding to target molecules. Cellular uptake and passive accumulation in tumors is also observed, as with folate incorporated silica nanoparticles loaded with perfluoropentane for prostate cancer.[182] Based on composition, there are three kinds of nanoparticle contrast agents currently in use for US imaging. The first type uses gas (microbubble) to create strong acoustic reflections, and is the most common material to be made into US contrast agents. These microbubbles include nitrogen, carbon dioxide, perfluorocarbon and sulfur hexafluoride.[183] Nanoparticles include liposomes, silica nanoparticles and polymer nanoparticles.[180, 184, 185] The second type uses a solid based nanoparticle design with relatively high scattering acoustic signals, often mediated by nanoparticle shape.[186] These nanoparticles are smaller than the gas-based particles, and accumulate in target lesions by cellular uptake, the EPR effect or specific receptor binding. An example includes the rattle-typed mesoporous silica nanostructure which has a powerful ultrasound signal in tumor.[187]

The final type is a liquid based nanoparticle. Perfluorooctyl bromide (PFOB) nanoparticles, for example, generate an acoustic signal due to a lower speed of sound transmission than that of water, and the shell also has intrinsic acoustic reflection.[188] Both gas and liquid based nanoparticles have the same core-shell structure, with the gas and liquid comprising the core.

5.3 Application in biomedical imaging

Nanoparticles as ultrasound contrast agents are much smaller than currently used ultrasound contrast agents. As other nanoparticles, the small size and additional surface labelling facilitate lesion targeting, as demonstrated with folate-PEG-chitosan loaded PFOB.[177] Not only as blood pool contrast agents, they can also provide strong signals in local target lesions, especially for tumor detection. Other applications include stem cell imaging, inflammation detection, and drug delivery.[189] Examples of nanoparticle ultrasound contrast agents in the literatures are summarized in Table 4, including nanoparticle composition and classification, nanoparticle size, biomedical applications, and whether the concept has been shown in vivo or in vitro.

5.4 Examples used in ultrasound imaging

There are three ways to load gases in the core of nanoparticles. The first method uses natural gas loaded in the nanoparticle core, including nitrogen, air, perfluorocarbon and sulfur hexafluoride.[180, 184] The second method uses phase transition from liquid to gas. When nanoparticles accumulate in the target lesion through active or passive mechanisms, the liquid in the nanoparticle core is stimulated by ultrasound waves to vaporize into gas to produce a strong acoustic reflection. This technique is used with AuNP coated/perfluorohexane encapsulated/PEGylated mesoporous silica nanocapsules.[178] The third method uses a chemical reaction to produce gas, commonly using carbonate. Carbonate, typically insoluble at neutral pH, is encapsulated in nanoparticles and can accumulate in tumors through the EPR effect or specific binding. Then, the acidic environment of the tumor reacts with the carbonate core to generate carbon dioxide gas for strong acoustic contrast. An example includes poly (cholesteryl carbonate γ-butyrolactone-propylene oxide) nanoparticles for tumor imaging (Fig. 7).[190] Ammonium bicarbonate has also demonstrated similar properties in acoustic imaging. [195]

6 Nanoparticles in PET/SPECT imaging applications

6.1 Advantages and limits of PET/SPECT

Positron emission tomography (PET) is a powerful and widely used nuclear medicine technology with high tissue penetration, high sensitivity and real-time quantitative imaging analysis. Besides anatomic information, PET may also provide biological information at the molecular level based on nuclide tracking. Single photon emission computed tomography (SPECT) is another widely used nuclear medicine technology with similar advantages as PET imaging, they can detect abnormal biochemical function before changes in anatomy. Limitations of PET/SPECT include high cost and radioactive exposure.

6.2 Structure and composition features

Nuclides with a reasonably long half-life are needed for nanoparticle PET/SPECT imaging tracers. The commonly used radioisotope for PET in clinical practice is Fluorine-18 with a half-life of 109.8 minutes, which is generally too short to apply in nanoparticles due to the time needed for preparation and cellular uptake.[196] Thus, other nuclides with longer half-lives are needed to prepare various nanoparticles. Examples include copper-64 with a half-life of 12.7 hours, Indium-111 with a half-life of 2.8 days and Iodine-124 with a half-life of 4.2 days.[197–199] With the exception of incorporation of a radionuclide tracer, nanoparticles for PET imaging are similar in structure to other described nanoparticles used for medical imaging. Compared with PET, radionuclides in SPECT generally have longer half-lives. The common radionuclide for SPECT in clinical use is Technetium-99m with a half-life of 6 hours. Nanoparticle structures for SPECT imaging are similar to structures for PET imaging. For example, Technetium-99m labeled macro-aggregated albumin particles are commonly used to quantify tumor volumes and pulmonary shunt fractions in the liver.[200] Other radionuclides used in nanoparticles [201] include Indium-111, Iodine-123, 125 and 131, and Gold-198, 199.

6.3 Application in biomedical imaging

Nanoparticles in PET/SPECT are mainly used in tumor detection. Tumor imaging can occur through specific binding to receptors or via the EPR effect.[198, 202] Imaging also can be acquired through active and passive accumulation in target lesions. Examples include vector tracking, atherosclerotic plaque imaging, and pharmacokinetic change of particles.[203] Examples of nanoparticles used in PET/SPECT imaging in the literature are summarized in Table 5, including, nanoparticle composition, size, biomedical applications, and whether the concept has been tested in vivo or in vitro.

6.4 Examples used in PET/SPECT imaging

Radiopharmaceutical nuclides are the essential element for nuclear medicine imaging; however, detachment of radiolabeled probes from nanoparticles can be a significant problem. Direct conjugation of nuclides to stable nanoparticles have addressed this problem for targeted imaging by PET (Fig. 8). Nanoparticles synthesized using poly(4-vinylphenol) (PVPh) polymer radiolabeled ^{124}I and surface-coated antibodies targeting endothelium have been used as a stable PET imaging platform facilitating image tracking in a translational model.[204]

7. Nanoparticles in multimodality imaging applications

7.1 Advantages and limits of multimodality imaging

The above described single imaging modalities have individual advantages and limits. For example, fluorescence imaging provides the best spatial resolution, but has limited tissue penetration. PET is extremely sensitive, has sufficient tissue penetration, and also provides functional information at the molecular level, but suffers from limited spatial resolution. CT provides excellent spatial resolution, but includes ionizing radiation. To overcome these limitations, interest in multimodality imaging methods has increased.[49, 205] Multifunctional

nanoparticles have been developed to offer multimodality imaging capabilities, with the potential benefits of reduced dose of contrast agent and more targeting ability. For example, a multimodality platform of ^{64}Cu-Fe-RGD-PEG-MNP can serve as a photoacoustic contrast agent, a PET contrast agent and an MRI imaging contrast agent.[5] Fluorescein isothiocyanate (FI) conjugated PEGylated gold nanoparticles are a biocompatible platform with both fluorescence and CT imaging capabilities.[49] Meanwhile, several limits need further investigation, which include various and different designs make them difficult to set a standard criteria, multimodality imaging is a relative new modality and there is a long journey to move it to clinical practice, special equipment with multiple imaging modules should be developed for further application.

7.2 Structure and composition features

The synthesis of multifunctional nanoplatforms is generally more complicated than that needed for single imaging modality nanoplatforms. Some multifunctional nanoparticles contain one imaging agent which can have dual imaging capabilities. Examples include silicon naphthalocyanine, that can serve as both an NIR fluorescence imaging agent and a photoacoustic imaging agent,[63] and Gd_2O_3, which has the potential for both CT and MRI imaging properties.[213] Most nanoparticles for multimodality imaging, however, contain more than one imaging material for different imaging modalities, such as iron oxide with dye (NIR830) in nanoparticles to provide MRI and fluorescence imaging, respectively.[214] Additionally, they can demonstrate any form of currently available nanostructure. Multifunctional nanoplatforms include MRI-fluorescence (Fig. 9),[215] MRI-PET, CT-fluorescence, CT-PET, MRI-US, MRI-CT, MRI-CT-fluorescence, MRI-PET-fluorescence, US-CT-MRI-fluorescence and PET-fluorescence.[167, 216–220]

7.3 Application in biomedical imaging

Due to the capability of nanoparticles for multimodality imaging, use in early tumor detection has garnered significant interest.[48, 221] Additional applications of multimodality nanoparticle-based imaging for the cardiovascular, renal, neural, and lymphatic systems have also been explored.[214, 219, 222, 223]

7.4 Examples used in multimodality imaging

Photoacoustic imaging is a hybrid optical and ultrasound biomedical imaging modality, which has the advantages of high contrast resolution and excellent spatial resolution based on optical imaging properties and deeper issue penetration based on ultrasound imaging properties. The photoacoustic signal is generated from the conversion of absorbed optical energy to ultrasound emission in a biological tissue with or without extraneous contrast agents.[224] The key point is the local temperature rise and thermoelastic expansion in tissue when irradiated by a nonionizing pulse laser. Due to the heat production during this process, photoacoustic imaging is often combined with photothermal therapy.[225]

While endogenous compounds including hemoglobin and melanin can be utilized as photoacoustic agents,[5] nanoparticles as exogenous contrast agents have increased development of photoacoustic imaging. Currently, one group of widely developed nanoparticles as photoacoustic contrast agents are inorganic materials, which include metal

nanoparticles (gold, silver, copper), and carbon nanomaterials including carbon nanotubes and graphene.[226–228] Another group of nanoparticles are organic materials based on small molecule dyes, such as indocyanine green and silicon naphthalocyanine.[63, 229] Other nanoparticles use microbubble production to generate acoustic waves after laser irradiation, such as CO_2 and N_2. Furthermore, photoacoustic imaging nanoparticles also can be synthesized by two or more materials from different groups, including indocyanine green-loaded silver nanoparticles and silver nanoparticles encapsulated with N_2 microbubbles.[230, 231]

For metal nanoparticles, surface plasmon resonance (SPR) is an important property to absorb light energy and produce heat when the light photons match the frequency of nanoparticle surface electron vibration. So these nanoparticles have been deeply investigated as photoacoustic imaging agents, especially for gold nanoparticles. The SPR peak wavelengths of current spherical gold nanoparticles are only 500 to 600 nm. Other shapes and surface decoration of gold nanoparticles have been developed in order to tune the peak SPR wavelength to the NIR spectrum. For example, gold nanorods, nanocages and nanoshells can be used as efficient photoacoustic imaging agents.[232–234] For carbon nanomaterials, low heat capacity and excellent light absorption make them possible to produce a photoacoustic signal, but the work is still preliminary.[235] Inorganic materials with inherent photoacoustic imaging properties can be formed into nanoparticles with relatively simple structures supplemented with surface labeling using antibodies and ligands (Fig. 5A). For example, MAGE targeted gold nanorods can be used to image melanoma.[236] Organic dyes as photoacoustic agents can be encapsulated into nanoparticles in the form of core-shell structures (Fig. 5B), and also can be decorated on the surface to form a vector structure (Fig. 5C). Examples include micelle encapsulated silicon naphthalocyanine and indocyanine green conjugated to the surface of albumin based nanoparticles.[63, 229] Other materials like gas or gas-generating materials also can be encapsulated into core-shell nanoparticles to play photoacoustic imaging functions, such as NH_4HCO_3 gas–generating liposomal nanoparticle for photoacoustic imaging in breast cancer.[195] For biomedical applications, nanoparticles as photoacoustic agents are mainly used in tumor imaging, with additional uses for cell tracking, lymph node imaging, vascular imaging, early detection of osteoarthritis and monitoring blood-brain barrier function.[221, 228, 237, 238]

8. Conclusions and perspective

In this review, we have illustrated structure-related properties and applications of nanoparticles in each biomedical imaging modality, including fluorescence imaging, MRI, CT, US, PET and SPECT. Compared to conventional contrast agents, nanoparticles have demonstrated improved signal intensity, targeting ability and longer circulation time both in vitro and in animal disease models, especially for cancer diagnosis and therapy. With the help of nanotechnology, single imaging modalities have become more powerful than before, and multimodality imaging has demonstrated significant promise.

There are currently about 50 nanodrugs that have been approved by the FDA.[239] Major sources of delay for translation to clinical practice involve the biodistribution and safety considerations of developed nanotechnology. Factors impacting nanoparticle biodistribution

include size, shape, surface charge and surface labeling.[240, 241] As illustrated before, nanoparticle size plays a particularly important role in biodistribution, Furthermore, the toxicity produced from nanoparticles after metabolism is still not fully understood. Some elements may bring damage to normal cells depending on the inherent physiochemical properties of nanoparticles. For example, the freedom state rare earth elements from quantum dots are harmful. Although encapsulation and surface labelling has been explored to reduce toxic effects, more work is needed to fully understand the behavior of nanoparticles in the future.[55]

A potential exciting role for nanoparticle imaging agents incorporates diagnostics with therapeutics in the same nanoplatform, termed theranostics (Fig. 10).[242] As delivery vehicles, nanoparticles have great potential to encapsulate various therapeutic agents to target locations at the time of biomedical imaging. In the past few years, many therapeutic methods have been investigated to integrate into theranostic nanoplatforms, including chemotherapy, photothermal therapy, radiation therapy, photodynamic therapy, immunotherapy and gene therapy.[168, 243–246] This strategy has been mainly used in tumor-related research.[14] As an example, ball-in-ball ZrO_2 nanoparticles can provide simultaneous CT imaging, and also have the function of synergistic microwave ablation and chemotherapy when accumulated in tumors.[165] To date, no theranostic nanoparticle has been approved by the FDA, partially due to significant heterogeneity in the design and synthesis of these agents. A significant effort in this field will be required in the future.

To maximize clinical translation of nanoparticle research, all features of the nanoparticles should be comprehensively understood, including composition, formulation, shape, surface charge, hydrodynamic diameter, solubility, stability, administration route, distribution, metabolism, clearance and potential toxic effects.[247] Rigorous study for safety and efficacy in well-designed clinical trials will be a challenging yet essential part of this evolution.[248] It takes an average of 12 years for a new drug to advance from invention to clinical application with FDA approval, and safety remains a critical aspect of this process.[249] Currently, most nano-contrast agents are still in the experiment stage. Despite the impressive progress that has been made, very few nano-contrast agents have been evaluated in humans. Ongoing development of nanoparticle research should focus on improving targeting specificity while minimizing toxicity. In addition, the importance of increasing translational potential with appropriate animal models cannot be overemphasized, along with understanding the specific pharmacokinetic profile of these agents in humans. Effective development of nanoparticles for biomedical imaging will require multidisciplinary teams of chemists, pharmacists, biologists, physicists, engineers and physicians. Despite these challenges, nanoparticles promise revolutionary potential as new imaging agents for a variety of clinical applications.

Acknowledgements

The research was funded by National Natural Science Foundation of China (NSFC) (No. 81630053), and in part by the Research Grants Program from the OSU Division of Health Sciences, NIH/NCATS KL2 Career Development Award KL2 TR002370 through Oregon Clinical and Translational Research Institute.

Notes and references:

1. Jung DH, Hwang S, Song GW, Ahn CS, Moon DB, Ha TY, Kim KH, Park GC, Kim BS, Park IJ, Lim SB, Kim JC, Yoo MW, Byeon JS, Jung HY, Lee GH, Myung SJ, Choe J, Choi JY, Park HW and Lee SG, Transplant Proc, 2016, 48, 145–151. [PubMed: 26915860]
2. Lu WL, Jansen L, Post WJ, Bonnema J, Van de Velde JC and De Bock GH, Breast Cancer Res Treat, 2009, 114, 403–412. [PubMed: 18421576]
3. Ryvolova M, Chomoucka J, Drbohlavova J, Kopel P, Babula P, Hynek D, Adam V, Eckschlager T, Hubalek J, Stiborova M, Kaiser J and Kizek R, Sensors (Basel), 2012, 12, 14792–14820.
4. Torres Martin de Rosales R, Tavare R, Glaria A, Varma G, Protti A and Blower PJ, Bioconjug Chem, 2011, 22, 455–465. [PubMed: 21338098]
5. Fan Q, Cheng K, Hu X, Ma X, Zhang R, Yang M, Lu X, Xing L, Huang W, Gambhir SS and Cheng Z, J Am Chem Soc, 2014, 136, 15185–15194.
6. Cuccurullo V, Di Stasio GD, Mazzarella G and Cascini GL, Contrast Media Mol Imaging, 2018, 2018, 9487938.
7. Chronos NA, Goodall AH, Wilson DJ, Sigwart U and Buller NP, Circulation, 1993, 88, 2035–2044. [PubMed: 8222096]
8. Petrik M, Weigel C, Kirsch M and Hosten N, Rofo, 2005, 177, 1242–1249. [PubMed: 16123870]
9. Oh IH, Min HS, Li L, Tran TH, Lee YK, Kwon IC, Choi K, Kim K and Huh KM, Biomaterials, 2013, 34, 6454–6463. [PubMed: 23755832]
10. Hoshyar N, Gray S, Han H and Bao G, Nanomedicine (Lond), 2016, 11, 673–692. [PubMed: 27003448]
11. Scott RP and Quaggin SE, J Cell Biol, 2015, 209, 199–210. [PubMed: 25918223]
12. Longmire M, Choyke PL and Kobayashi H, Nanomedicine (Lond), 2008, 3, 703–717. [PubMed: 18817471]
13. Zhou Y and Dai Z, Chem Asian J, 2018, DOI: 10.1002/asia.201800149.
14. Huang Y, He S, Cao W, Cai K and Liang X-J, Nanoscale, 2012, 4, 6135–6149. [PubMed: 22929990]
15. Chen LQ, Xiao SJ, Hu PP, Peng L, Ma J, Luo LF, Li YF and Huang CZ, Anal Chem, 2012, 84, 3099–3110. [PubMed: 22423600]
16. Das M, Duan W and Sahoo SK, Nanomedicine, 2015, 11, 379–389. [PubMed: 25240596]
17. Ke R, Yang W, Xia X, Xu Y and Li Q, Anal Biochem, 2010, 406, 8–13. [PubMed: 20599640]
18. Kim D, Jeong YY and Jon S, ACS Nano, 2010, 4, 3689–3696. [PubMed: 20550178]
19. Wang Z, Qiao R, Tang N, Lu Z, Wang H, Zhang Z, Xue X, Huang Z, Zhang S, Zhang G and Li Y, Biomaterials, 2017, 127, 25–35. [PubMed: 28279919]
20. Alibakhshi A, Abarghooi Kahaki F, Ahangarzadeh S, Yaghoobi H, Yarian F, Arezumand R, Ranjbari J, Mokhtarzadeh A and de la Guardia M, J Control Release, 2017, 268, 323–334. [PubMed: 29107128]
21. Jo H and Ban C, Exp Mol Med, 2016, 48, e230. [PubMed: 27151454]
22. Alshaer W, Hillaireau H and Fattal E, Adv Drug Deliv Rev, 2018, DOI: 10.1016/j.addr.2018.09.011.
23. He F, Wen N, Xiao D, Yan J, Xiong H, Cai S, Liu Z and Liu Y, Curr Med Chem, 2018, DOI: 10.2174/0929867325666181008142831.
24. Inaba H and Matsuura K, Chem Rec, 2018, DOI: 10.1002/tcr.201800149.
25. Bellis SL, Biomaterials, 2011, 32, 4205–4210. [PubMed: 21515168]
26. Li Y, Xiao Y, Lin HP, Reichel D, Bae Y, Lee EY, Jiang Y, Huang X, Yang C and Wang Z, Biomaterials, 2018, 188, 160–172. [PubMed: 30352320]
27. Zhong Y, Meng F, Deng C and Zhong Z, Biomacromolecules, 2014, 15, 1955–1969. [PubMed: 24798476]
28. Yu X, Trase I, Ren M, Duval K, Guo X and Chen Z, J Nanomater, 2016, 2016, DOI:10.1155/2016/1087250.

29. Wang A, Yin L, He L, Xia H, Chen F, Zhao M, Ding J and Shi H, Nanoscale, 2018, 10, 20126–20130.
30. Yang L, Sun H, Liu Y, Hou W, Yang Y, Cai R, Cui C, Zhang P, Pan X, Li X, Li L, Sumerlin B and Tan W, Angew Chem Int Ed Engl, 2018, DOI: 10.1002/anie.201809753.
31. Wang JL, Du XJ, Yang JX, Shen S, Li HJ, Luo YL, Iqbal S, Xu CF, Ye XD, Cao J and Wang J, Biomaterials, 2018, 182, 104–113. [PubMed: 30114562]
32. Hu J, Sheng Y, Shi J, Yu B, Yu Z and Liao G, Curr Drug Metab, 2018, 19, 723–738. [PubMed: 29219050]
33. Mozar FS and Chowdhury EH, J Pharm Sci, 2018, 107, 2497–2508. [PubMed: 29883662]
34. Abdollah MRA, Carter TJ, Jones C, Kalber TL, Rajkumar V, Tolner B, Gruettner C, Zaw-Thin M, Baguna Torres J, Ellis M, Robson M, Pedley RB, Mulholland P, d. R. R TM and Chester KA, ACS Nano, 2018, 12, 1156–1169. [PubMed: 29341587]
35. Mustafa S, Devi VK and Pai RS, Drug Deliv Transl Res, 2017, 7, 27–36. [PubMed: 27576453]
36. Liu X, Li H, Chen Y, Jin Q, Ren K and Ji J, Adv Healthc Mater, 2014, 3, 1439–1447. [PubMed: 24550205]
37. Xiao W, Lin J, Li M, Ma Y, Chen Y, Zhang C, Li D and Gu H, Contrast Media Mol Imaging, 2012, 7, 320–327. [PubMed: 22539402]
38. Esfandyari-Manesh M, Mostafavi SH, Majidi RF, Koopaei MN, Ravari NS, Amini M, Darvishi B, Ostad SN, Atyabi F and Dinarvand R, Daru, 2015, 23, 28. [PubMed: 25903677]
39. Bakhtiary Z, Saei AA, Hajipour MJ, Raoufi M, Vermesh O and Mahmoudi M, Nanomedicine, 2016, 12, 287–307. [PubMed: 26707817]
40. Zhao Y, Pang B, Detering L, Luehmann H, Yang M, Black K, Sultan D, Xia Y and Liu Y, Mol Imaging, 2018, 17, 1536012118775827.
41. Tao Y, Li M, Kim B and Auguste DT, Theranostics, 2017, 7, 899–911. [PubMed: 28382162]
42. Coutinho C and Somoza A, Anal Bioanal Chem, 2018, DOI: 10.1007/s00216-018-1450-7.
43. Li R, Liu B and Gao J, Cancer Lett, 2017, 386, 123–130. [PubMed: 27845158]
44. Salahandish R, Ghaffarinejad A, Omidinia E, Zargartalebi H, Majidzadeh AK, Naghib SM and Sanati-Nezhad A, Biosens Bioelectron, 2018, 120, 129–136. [PubMed: 30172235]
45. Hasanzadeh M, Solhi E, Jafari M, Mokhtarzadeh A, Soleymani J, Jouyban A and Mahboob S, International journal of biological macromolecules, 2018, 120, 2493–2508. [PubMed: 30195002]
46. Huang Q, Wang Y, Chen X, Wang Y, Li Z, Du S, Wang L and Chen S, Nanotheranostics, 2018, 2, 21–41. [PubMed: 29291161]
47. Montet X, Montet-Abou K, Reynolds F, Weissleder R and Josephson L, Neoplasia, 2006, 8, 214–222. [PubMed: 16611415]
48. Montet X, Weissleder R and Josephson L, Bioconjug Chem, 2006, 17, 905–911. [PubMed: 16848396]
49. Qin J, Peng C, Zhao B, Ye K, Yuan F, Peng Z, Yang X, Huang L, Jiang M, Zhao Q, Tang G and Lu X, Int J Nanomedicine, 2014, 9, 5575–5590. [PubMed: 25506213]
50. Winter PM, Caruthers SD, Kassner A, Harris TD, Chinen LK, Allen JS, Lacy EK, Zhang H, Robertson JD, Wickline SA and Lanza GM, Cancer Res, 2003, 63, 5838–5843. [PubMed: 14522907]
51. Lee H, Sung D, Kim J, Kim BT, Wang T, An SS, Seo SW and Yi DK, Int J Nanomedicine, 2015, 10 Spec Iss, 215–225. [PubMed: 26357472]
52. Jackson P, Periasamy S, Bansal V and Geso M, Australas Phys Eng Sci Med, 2011, 34, 243–249. [PubMed: 21465276]
53. Bhavane R, Badea C, Ghaghada KB, Clark D, Vela D, Moturu A, Annapragada A, Johnson GA, Willerson JT and Annapragada A, Circ Cardiovasc Imaging, 2013, 6, 285–294. [PubMed: 23349231]
54. Nune SK, Gunda P, Thallapally PK, Lin YY, Forrest ML and Berkland CJ, Expert Opin Drug Deliv, 2009, 6, 1175–1194. [PubMed: 19743894]
55. Lewinski N, Colvin V and Drezek R, Small, 2008, 4, 26–49. [PubMed: 18165959]

56. Santra S and Malhotra A, Wiley Interdiscip Rev Nanomed Nanobiotechnol, 2011, 3, 501–510. [PubMed: 21480546]
57. Foucault-Collet A, Gogick KA, White KA, Villette S, Pallier A, Collet G, Kieda C, Li T, Geib SJ, Rosi NL and Petoud S, Proc Natl Acad Sci U S A, 2013, 110, 17199–17204.
58. Hwang ES, Cao C, Hong S, Jung HJ, Cha CY, Choi JB, Kim YJ and Baik S, Nanotechnology, 2006, 17, 3442–3445. [PubMed: 19661588]
59. Cai Z, Ye Z, Yang X, Chang Y, Wang H, Liu Y and Cao A, Nanoscale, 2011, 3, 1974–1976. [PubMed: 21369623]
60. Genovese D, Bonacchi S, Juris R, Montalti M, Prodi L, Rampazzo E and Zaccheroni N, Angew Chem Int Ed Engl, 2013, 52, 5965–5968. [PubMed: 23616475]
61. Grebenik EA, Nadort A, Generalova AN, Nechaev AV, Sreenivasan VK, Khaydukov EV, Semchishen VA, Popov AP, Sokolov VI, Akhmanov AS, Zubov VP, Klinov DV, Panchenko VY, Deyev SM and Zvyagin AV, J Biomed Opt, 2013, 18, 76004.
62. Fan Z, Senapati D, Singh AK and Ray PC, Mol Pharm, 2013, 10, 857–866. [PubMed: 23110457]
63. Taratula O, Doddapaneni BS, Schumann C, Li X, Bracha S, Milovancev M, Alani AWG and Taratula O, Chemistry of Materials, 2015, 27, 6155–6165.
64. Taratula O, Schumann C, Duong T, Taylor KL and Taratula O, Nanoscale, 2015, 7, 3888–3902. [PubMed: 25422147]
65. Santra S, Dutta D, Walter GA and Moudgil BM, Technol Cancer Res Treat, 2005, 4, 593–602. [PubMed: 16292879]
66. Henderson L, Neumann O, Kaffes C, Zhang R, Marangoni V, Ravoori MK, Kundra V, Bankson J, Nordlander P and Halas NJ, ACS Nano, 2018, 12, 8214–8223. [PubMed: 30088917]
67. Lee S, Cha EJ, Park K, Lee SY, Hong JK, Sun IC, Kim SY, Choi K, Kwon IC, Kim K and Ahn CH, Angew Chem Int Ed Engl, 2008, 47, 2804–2807. [PubMed: 18306196]
68. Sun IC, Lee S, Koo H, Kwon IC, Choi K, Ahn CH and Kim K, Bioconjug Chem, 2010, 21, 1939–1942. [PubMed: 20936793]
69. Chen LJ, Sun SK, Wang Y, Yang CX, Wu SQ and Yan XP, ACS Appl Mater Interfaces, 2016, 8, 32667–32674.
70. Li L, Feng J, Fan Y and Tang B, Anal Chem, 2015, 87, 4829–4835. [PubMed: 25853631]
71. Pillai SS, Yukawa H, Onoshima D, Biju V and Baba Y, Anal Sci, 2017, 33, 137–142. [PubMed: 28190830]
72. Chen NT, Cheng SH, Liu CP, Souris JS, Chen CT, Mou CY and Lo LW, Int J Mol Sci, 2012, 13, 16598–16623.
73. Kim D, Lee N, Park YI and Hyeon T, Bioconjug Chem, 2017, 28, 115–123. [PubMed: 27982578]
74. Yu K, Zaman B and Ripmeester JA, J Nanosci Nanotechnol, 2005, 5, 669–681. [PubMed: 16004136]
75. Mokoena TP, Linganiso EC, Kumar V, Swart HC, Cho SH and Ntwaeaborwa OM, Journal of colloid and interface science, 2017, 496, 87–99. [PubMed: 28214627]
76. Ryu JH, Lee A, Chu JU, Koo H, Ko CY, Kim HS, Yoon SY, Kim BS, Choi K, Kwon IC, Kim K and Youn I, Arthritis Rheum, 2011, 63, 3824–3832. [PubMed: 22127700]
77. Wei Y, Chen Q, Wu B, Zhou A and Xing D, Nanoscale, 2012, 4, 3901–3909. [PubMed: 22652931]
78. Muthukumar T, Chamundeeswari M, Prabhavathi S, Gurunathan B, Chandhuru J and Sastry TP, Eur J Pharm Biopharm, 2014, 88, 730–736. [PubMed: 25305584]
79. Wang Y, Zhou K, Huang G, Hensley C, Huang X, Ma X, Zhao T, Sumer BD, DeBerardinis RJ and Gao J, Nat Mater, 2014, 13, 204–212. [PubMed: 24317187]
80. Markovic S, Belz J, Kumar R, Cormack RA, Sridhar S and Niedre M, Int J Nanomedicine, 2016, 11, 1213–1223. [PubMed: 27069363]
81. Dubreil L, Leroux I, Ledevin M, Schleder C, Lagalice L, Lovo C, Fleurisson R, Passemard S, Kilin V, Gerber-Lemaire S, Colle MA, Bonacina L and Rouger K, ACS Nano, 2017, 11, 6672–6681. [PubMed: 28644009]
82. Naseri N, Ajorlou E, Asghari F and Pilehvar-Soltanahmadi Y, Artif Cells Nanomed Biotechnol, 2017, DOI: 10.1080/21691401.2017.1379014, 1–11.

83. Segets D, Lucas JM, Klupp Taylor RN, Scheele M, Zheng H, Alivisatos AP and Peukert W, ACS Nano, 2012, 6, 9021–9032. [PubMed: 22984808]
84. Thiruppathi R, Mishra S, Ganapathy M, Padmanabhan P and Gulyas B, Adv Sci (Weinh), 2017, 4, 1600279.
85. Zhao Y, van Rooy I, Hak S, Fay F, Tang J, Davies Cde L, Skobe M, Fisher EA, Radu A, Fayad ZA, de Mello Donega C, Meijerink A and Mulder WJ, ACS Nano, 2013, 7, 10362–10370.
86. Klanjscek T, Nisbet RM, Priester JH and Holden PA, Ecotoxicology, 2013, 22, 319–330. [PubMed: 23291788]
87. Gao J, Chen K, Luong R, Bouley DM, Mao H, Qiao T, Gambhir SS and Cheng Z, Nano Lett, 2012, 12, 281–286. [PubMed: 22172022]
88. Savla R, Taratula O, Garbuzenko O and Minko T, J Control Release, 2011, 153, 16–22. [PubMed: 21342659]
89. Wu Y, Eisele K, Doroshenko M, Algara-Siller G, Kaiser U, Koynov K and Weil T, Small, 2012, 8, 3465–3475. [PubMed: 22915540]
90. Adegoke O, Seo MW, Kato T, Kawahito S and Park EY, Biosens Bioelectron, 2016, 86, 135–142. [PubMed: 27348778]
91. Meledandri CJ, Stolarczyk JK and Brougham DF, ACS Nano, 2011, 5, 1747–1755. [PubMed: 21309572]
92. Sardar R and Shumaker-Parry JS, J Am Chem Soc, 2011, 133, 8179–8190. [PubMed: 21548572]
93. Mesbahi A, Jamali F and Garehaghaji N, Bioimpacts, 2013, 3, 29–35. [PubMed: 23678467]
94. Geng J, Li K, Pu KY, Ding D and Liu B, Small, 2012, 8, 2421–2429. [PubMed: 22544732]
95. Zhang P, Wang Y, Leng F, Xiong ZH and Huang CZ, Talanta, 2013, 112, 117–122. [PubMed: 23708546]
96. Gao L, Lian C, Zhou Y, Yan L, Li Q, Zhang C, Chen L and Chen K, Biosens Bioelectron, 2014, 60, 22–29. [PubMed: 24768760]
97. Pan XW, Liu N, Zheng DX, Shi MM, Wu G, Wang M and Chen HZ, Nanotechnology, 2009, 20, 415605.
98. Zhu S, Liu Z, Hu L, Yuan Y and Xu G, Chemistry, 2012, 18, 16556–16561.
99. Pang S, Gao Y, Li Y, Liu S and Su X, Analyst, 2013, 138, 2749–2754. [PubMed: 23505623]
100. Pillai SS, Yukawa H, Onoshima D, Biju V and Baba Y, Cell Med, 2015, 8, 57–62. [PubMed: 26858909]
101. Pu KY, Li K and Liu B, Adv Mater, 2010, 22, 643–646. [PubMed: 20217765]
102. Blechinger J, Herrmann R, Kiener D, Garcia-Garcia FJ, Scheu C, Reller A and Brauchle C, Small, 2010, 6, 2427–2435. [PubMed: 20878633]
103. Chen G, Jaskula-Sztul R, Esquibel CR, Lou I, Zheng Q, Dammalapati A, Harrison A, Eliceiri KW, Tang W, Chen H and Gong S, Adv Funct Mater, 2017, 27, DOI: 10.1002/adfm.201604671.
104. Iacono P, Karabeber H and Kircher MF, Angew Chem Int Ed Engl, 2014, 53, 11756–11761.
105. Zhang Y, Li X, Kang X, Hou Z and Lin J, Phys Chem Chem Phys, 2014, 16, 10779–10787.
106. Xiao Q, Zhang Y, Zhang H, Dong G, Han J and Qiu J, Sci Rep, 2016, 6, 31327.
107. Tikhomirov VK, Mortier M, Gredin P, Patriarche G, Gorller-Walrand C and Moshchalkov VV, Opt Express, 2008, 16, 14544–14549.
108. Babu S, Cho JH, Dowding JM, Heckert E, Komanski C, Das S, Colon J, Baker CH, Bass M, Self WT and Seal S, Chem Commun (Camb), 2010, 46, 6915–6917. [PubMed: 20683524]
109. Qu A, Wu X, Xu L, Liu L, Ma W, Kuang H and Xu C, Nanoscale, 2017, 9, 3865–3872. [PubMed: 28252127]
110. Zhang Y, Li X, Hou Z and Lin J, Nanoscale, 2014, 6, 6763–6771. [PubMed: 24827577]
111. Donato H, Franca M, Candelaria I and Caseiro-Alves F, Eur J Radiol, 2017, 93, 30–39. [PubMed: 28668428]
112. Bashir MR, Magn Reson Imaging Clin N Am, 2014, 22, 283–293. [PubMed: 25086930]
113. Ghaghada KB, Starosolski ZA, Bhayana S, Stupin I, Patel CV, Bhavane RC, Gao H, Bednov A, Yallampalli C, Belfort M, George V and Annapragada AV, Placenta, 2017, 57, 60–70. [PubMed: 28864020]

114. Vargo KB, Zaki AA, Warden-Rothman R, Tsourkas A and Hammer DA, Small, 2015, 11, 1409–1413. [PubMed: 25418741]
115. Thorek DL, Chen AK, Czupryna J and Tsourkas A, Ann Biomed Eng, 2006, 34, 23–38. [PubMed: 16496086]
116. Mekuria SL, Debele TA and Tsai HC, ACS Appl Mater Interfaces, 2017, 9, 6782–6795. [PubMed: 28164704]
117. Huang P, Guo W, Yang G, Song H, Wang Y, Wang C, Kong D and Wang W, ACS Appl Mater Interfaces, 2018, 10, 18532–18542.
118. Li N, Li S and Shen J, Front Phys, 2017, 5, DOI: 10.3389/fphy.2017.00026.
119. Sedivy P, Drobny M, Dezortova M, Herynek V, Roztocil K, Cermakova H, Nemcova A, Dubsky M and Hajek M, Int Angiol, 2018, 37, 293–299. [PubMed: 29644834]
120. Hou G, Byeon IJ, Ahn J, Gronenborn AM and Polenova T, J Am Chem Soc, 2011, 133, 18646–18655.
121. Suzuki K, Igarashi H, Huber VJ, Kitaura H, Kwee IL and Nakada T, J Neuroimaging, 2014, 24, 595–598. [PubMed: 25370340]
122. Yu YB, Wiley Interdiscip Rev Nanomed Nanobiotechnol, 2013, 5, 646–661. [PubMed: 23929813]
123. Zhang Z, Mascheri N, Dharmakumar R, Fan Z, Paunesku T, Woloschak G and Li D, Cytotherapy, 2009, 11, 43–51. [PubMed: 18956269]
124. Marangoni VS, Neumann O, Henderson L, Kaffes CC, Zhang H, Zhang R, Bishnoi S, Ayala-Orozco C, Zucolotto V, Bankson JA, Nordlander P and Halas NJ, Proc Natl Acad Sci U S A, 2017, 114, 6960–6965. [PubMed: 28630340]
125. Song Y, Xu X, MacRenaris KW, Zhang XQ, Mirkin CA and Meade TJ, Angew Chem Int Ed Engl, 2009, 48, 9143–9147. [PubMed: 19882611]
126. Ghaghada KB, Ravoori M, Sabapathy D, Bankson J, Kundra V and Annapragada A, PLoS One, 2009, 4, e7628.
127. Kolouchova K, Sedlacek O, Jirak D, Babuka D, Blahut J, Kotek J, Vit M, Trousil J, Konefal R, Janouskova O, Podhorska B, Slouf M and Hruby M, Biomacromolecules, 2018, 19, 3515–3524. [PubMed: 30011367]
128. Jun YW, Lee JH and Cheon J, Angew Chem Int Ed Engl, 2008, 47, 5122–5135. [PubMed: 18574805]
129. Frias JC, Ma Y, Williams KJ, Fayad ZA and Fisher EA, Nano Lett, 2006, 6, 2220–2224. [PubMed: 17034087]
130. Rahmer J, Antonelli A, Sfara C, Tiemann B, Gleich B, Magnani M, Weizenecker J and Borgert J, Phys Med Biol, 2013, 58, 3965–3977. [PubMed: 23685712]
131. Park IK, Ng CP, Wang J, Chu B, Yuan C, Zhang S and Pun SH, Biomaterials, 2008, 29, 724–732. [PubMed: 18006052]
132. Mi P, Kokuryo D, Cabral H, Wu H, Terada Y, Saga T, Aoki I, Nishiyama N and Kataoka K, Nat Nanotechnol, 2016, 11, 724–730. [PubMed: 27183055]
133. Keca JM, Chen J, Overchuk M, Muhanna N, MacLaughlin CM, Jin CS, Foltz WD, Irish JC and Zheng G, Angew Chem Int Ed Engl, 2016, 55, 6187–6191. [PubMed: 27071806]
134. Hu J, Qian Y, Wang X, Liu T and Liu S, Langmuir, 2012, 28, 2073–2082. [PubMed: 22047551]
135. Lanza GM, Yu X, Winter PM, Abendschein DR, Karukstis KK, Scott MJ, Chinen LK, Fuhrhop RW, Scherrer DE and Wickline SA, Circulation, 2002, 106, 2842–2847. [PubMed: 12451012]
136. Starmans LW, Moonen RP, Aussems-Custers E, Daemen MJ, Strijkers GJ, Nicolay K and Grull H, PLoS One, 2015, 10, e0119257.
137. Jin AY, Tuor UI, Rushforth D, Filfil R, Kaur J, Ni F, Tomanek B and Barber PA, Contrast Media Mol Imaging, 2009, 4, 305–311. [PubMed: 19941323]
138. Lu J, Ma S, Sun J, Xia C, Liu C, Wang Z, Zhao X, Gao F, Gong Q, Song B, Shuai X, Ai H and Gu Z, Biomaterials, 2009, 30, 2919–2928. [PubMed: 19230966]
139. Oishi K, Miyamoto Y, Saito H, Murase K, Ono K, Sawada M, Watanabe M, Noguchi Y, Fujiwara T, Hayashi S and Noguchi H, PLoS One, 2013, 8, e57046.

140. Hachani R, Birchall MA, Lowdell MW, Kasparis G, Tung LD, Manshian BB, Soenen SJ, Gsell W, Himmelreich U, Gharagouzloo CA, Sridhar S and Thanh NTK, Sci Rep, 2017, 7, 7850. [PubMed: 28798327]
141. Wang AZ, Bagalkot V, Vasilliou CC, Gu F, Alexis F, Zhang L, Shaikh M, Yuet K, Cima MJ, Langer R, Kantoff PW, Bander NH, Jon S and Farokhzad OC, ChemMedChem, 2008, 3, 1311–1315. [PubMed: 18613203]
142. Zhang C, Moonshi SS, Wang W, Ta HT, Han Y, Han FY, Peng H, Kral P, Rolfe BE, Gooding JJ, Gaus K and Whittaker AK, ACS Nano, 2018, 12, 9162–9176. [PubMed: 30118590]
143. Shen Z, Wu A and Chen X, Mol Pharm, 2017, 14, 1352–1364. [PubMed: 27776215]
144. Hogemann D, Ntziachristos V, Josephson L and Weissleder R, Bioconjug Chem, 2002, 13, 116–121. [PubMed: 11792186]
145. Liu G, Wang Z, Lu J, Xia C, Gao F, Gong Q, Song B, Zhao X, Shuai X, Chen X, Ai H and Gu Z, Biomaterials, 2011, 32, 528–537. [PubMed: 20869767]
146. Vilarino-Varela MJ, Taylor A, Rockall AG, Reznek RH and Powell ME, Radiother Oncol, 2008, 89, 192–196. [PubMed: 18771811]
147. Tromsdorf UI, Bigall NC, Kaul MG, Bruns OT, Nikolic MS, Mollwitz B, Sperling RA, Reimer R, Hohenberg H, Parak WJ, Forster S, Beisiegel U, Adam G and Weller H, Nano Lett, 2007, 7, 2422–2427. [PubMed: 17658761]
148. Jeon TY, Kim JH, Im GH, Kim JH, Yang J, Yoo SY and Lee JH, Br J Radiol, 2016, 89, 20150806.
149. Romero-Aburto R, Narayanan TN, Nagaoka Y, Hasumura T, Mitcham TM, Fukuda T, Cox PJ, Bouchard RR, Maekawa T, Kumar DS, Torti SV, Mani SA and Ajayan PM, Adv Mater, 2013, 25, 5632–5637. [PubMed: 24038195]
150. Hu YH, Small, 2014, 10, 1451–1452. [PubMed: 24376224]
151. Taylor RM, Huber DL, Monson TC, Esch V and Sillerud LO, J Vac Sci Technol B Nanotechnol Microelectron, 2012, 30, 2C101–102C1016.
152. Xu X, Zhang R, Liu F, Ping J, Wen X, Wang H, Wang K, Sun X, Zou H, Shen B and Wu L, Nanomedicine (Lond), 2018, DOI: 10.2217/nnm-2018-0051.
153. Swider E, Daoudi K, Staal AHJ, Koshkina O, van Riessen NK, van Dinther E, de Vries IJM, de Korte CL and Srinivas M, Nanotheranostics, 2018, 2, 258–268. [PubMed: 29868350]
154. Akazawa K, Sugihara F, Minoshima M, Mizukami S and Kikuchi K, Chem Commun (Camb), 2018, 54, 11785–11788.
155. Bo S, Yuan Y, Chen Y, Yang Z, Chen S, Zhou X and Jiang ZX, Chem Commun (Camb), 2018, 54, 3875–3878. [PubMed: 29594281]
156. Ghaghada KB, Badea CT, Karumbaiah L, Fettig N, Bellamkonda RV, Johnson GA and Annapragada A, Acad Radiol, 2011, 18, 20–30. [PubMed: 21145026]
157. Bonitatibus PJ Jr., Torres AS, Goddard GD, FitzGerald PF and Kulkarni AM, Chem Commun (Camb), 2010, 46, 8956–8958. [PubMed: 20976321]
158. Ahn S, Jung SY, Seo E and Lee SJ, Biomaterials, 2011, 32, 7191–7199. [PubMed: 21777977]
159. Chien CC, Chen HH, Lai SF, Hwu Y, Petibois C, Yang CS, Chu Y and Margaritondo G, Sci Rep, 2012, 2, 610. [PubMed: 22934133]
160. Hainfeld JF, Smilowitz HM, O'Connor MJ, Dilmanian FA and Slatkin DN, Nanomedicine (Lond), 2013, 8, 1601–1609. [PubMed: 23265347]
161. Silvestri A, Zambelli V, Ferretti AM, Salerno D, Bellani G and Polito L, Contrast Media Mol Imaging, 2016, 11, 405–414. [PubMed: 27377033]
162. Samei E, Saunders RS, Badea CT, Ghaghada KB, Hedlund LW, Qi Y, Yuan H, Bentley RC and Mukundan S Jr., Int J Nanomedicine, 2009, 4, 277–282. [PubMed: 20011244]
163. Betzer O, Shwartz A, Motiei M, Kazimirsky G, Gispan I, Damti E, Brodie C, Yadid G and Popovtzer R, ACS Nano, 2014, 8, 9274–9285. [PubMed: 25133802]
164. Maiorano G, Mele E, Frassanito MC, Restini E, Athanassiou A and Pompa PP, Nanoscale, 2016, 8, 18921–18927.
165. Long D, Niu M, Tan L, Fu C, Ren X, Xu K, Zhong H, Wang J, Li L and Meng X, Nanoscale, 2017, 9, 8834–8847. [PubMed: 28632268]

166. Boote E, Fent G, Kattumuri V, Casteel S, Katti K, Chanda N, Kannan R, Katti K and Churchill R, Acad Radiol, 2010, 17, 410–417. [PubMed: 20207313]
167. Zeng C, Shang W, Liang X, Liang X, Chen Q, Chi C, Du Y, Fang C and Tian J, ACS Appl Mater Interfaces, 2016, 8, 29232–29241.
168. Tan L, Liu T, Fu C, Wang S, Fu S, Ren J and Meng X, J. Mater. Chem. B, 2016, 4, 859–866. [PubMed: 32263158]
169. Tian C, Zhu L, Lin F and Boyes SG, ACS Appl Mater Interfaces, 2015, 7, 17765–17775.
170. Shi H, Niu M, Tan L, Liu T, Shao H, Fu C, Ren X, Ma T, Ren J, Li L, Liu H, Xu K, Wang J, Tang F and Meng X, Chem. Sci, 2015, 6, 5016–5026. [PubMed: 30155006]
171. Ahn S, Jung SY and Lee SJ, Molecules, 2013, 18, 5858–5890. [PubMed: 23685939]
172. Zhu J, Sun W, Zhang J, Zhou Y, Shen M, Peng C and Shi X, Bioconjug Chem, 2017, 28, 2692–2697. [PubMed: 29083866]
173. Kee PH and Danila D, Nanomedicine, 2018, 14, 1941–1947. [PubMed: 29933021]
174. Wowra B, Mentrup E, Zeller WJ, Stricker H and Sturm V, Onkologie, 1988, 11, 81–84. [PubMed: 3041328]
175. Balcar I, Seltzer SE, Davis S and Geller S, Radiology, 1984, 151, 723–729. [PubMed: 6718733]
176. Danila D, Partha R, Elrod DB, Lackey M, Casscells SW and Conyers JL, Tex Heart Inst J, 2009, 36, 393–403. [PubMed: 19876414]
177. Hu Y, Wang Y, Jiang J, Han B, Zhang S, Li K, Ge S and Liu Y, Biomed Res Int, 2016, 2016, 6381464.
178. Wang X, Chen H, Zheng Y, Ma M, Chen Y, Zhang K, Zeng D and Shi J, Biomaterials, 2013, 34, 2057–2068. [PubMed: 23246067]
179. Sakamoto JH, Smith BR, Xie B, Rokhlin SI, Lee SC and Ferrari M, Technol Cancer Res Treat, 2005, 4, 627–636. [PubMed: 16292882]
180. Seo M, Gorelikov I, Williams R and Matsuura N, Langmuir, 2010, 26, 13855–13860.
181. Min KH, Min HS, Lee HJ, Park DJ, Yhee JY, Kim K, Kwon IC, Jeong SY, Silvestre OF, Chen X, Hwang YS, Kim EC and Lee SC, ACS Nano, 2015, 9, 134–145. [PubMed: 25559896]
182. Wang J, Barback CV, Ta CN, Weeks J, Gude N, Mattrey RF, Blair SL, Trogler WC, Lee H and Kummel AC, IEEE Trans Med Imaging, 2018, 37, 222–229. [PubMed: 28829305]
183. Lanza GM and Wickline SA, Prog Cardiovasc Dis, 2001, 44, 13–31. [PubMed: 11533924]
184. Wang CW, Yang SP, Hu H, Du J and Li FH, Mol Med Rep, 2015, 11, 1885–1890. [PubMed: 25394467]
185. Park SH, Yoon YI, Moon H, Lee GH, Lee BH, Yoon TJ and Lee HJ, Oncol Rep, 2016, 36, 131–136. [PubMed: 27220374]
186. Chen F, Ma M, Wang J, Wang F, Chern SX, Zhao ER, Jhunjhunwala A, Darmadi S, Chen H and Jokerst JV, Nanoscale, 2017, 9, 402–411. [PubMed: 27924340]
187. Zhang K, Chen H, Guo X, Zhang D, Zheng Y, Zheng H and Shi J, Sci Rep, 2015, 5, 8766. [PubMed: 25739832]
188. Flegg MB, Poole CM, Whittaker AK, Keen I and Langton CM, Phys Med Biol, 2010, 55, 3061–3076. [PubMed: 20463372]
189. Kim GW, Kang C, Oh YB, Ko MH, Seo JH and Lee D, Theranostics, 2017, 7, 2463–2476. [PubMed: 28744328]
190. Min HS, Son S, You DG, Lee TW, Lee J, Lee S, Yhee JY, Lee J, Han MH, Park JH, Kim SH, Choi K, Park K, Kim K and Kwon IC, Biomaterials, 2016, 108, 57–70. [PubMed: 27619240]
191. Liu J, Li J, Rosol TJ, Pan X and Voorhees JL, Phys Med Biol, 2007, 52, 4739–4747. [PubMed: 17671332]
192. Lee J, Min HS, You DG, Kim K, Kwon IC, Rhim T and Lee KY, J Control Release, 2016, 223, 197–206. [PubMed: 26739549]
193. Paproski RJ, Forbrich A, Huynh E, Chen J, Lewis JD, Zheng G and Zemp RJ, Small, 2016, 12, 371–380. [PubMed: 26633744]
194. Peyman SA, McLaughlan JR, Abou-Saleh RH, Marston G, Johnson BR, Freear S, Coletta PL, Markham AF and Evans SD, Lab on a chip, 2016, 16, 679–687. [PubMed: 26689151]

195. Xia J, Feng G, Xia X, Hao L and Wang Z, Int J Nanomedicine, 2017, 12, 1803–1813. [PubMed: 28293107]
196. Lee SB, Kim HL, Jeong HJ, Lim ST, Sohn MH and Kim DW, Angew Chem Int Ed Engl, 2013, 52, 10549–10552.
197. Zern BJ, Chacko AM, Liu J, Greineder CF, Blankemeyer ER, Radhakrishnan R and Muzykantov V, ACS Nano, 2013, 7, 2461–2469. [PubMed: 23383962]
198. Schluep T, Hwang J, Hildebrandt IJ, Czernin J, Choi CH, Alabi CA, Mack BC and Davis ME, Proc Natl Acad Sci U S A, 2009, 106, 11394–11399.
199. Zhang R, Huang M, Zhou M, Wen X, Huang Q and Li C, Mol Imaging, 2013, 12, 182–190. [PubMed: 23490444]
200. Veres DS, Mathe D, Futo I, Horvath I, Balazs A, Karlinger K and Szigeti K, Mol Imaging Biol, 2014, 16, 167–172. [PubMed: 23996677]
201. Black KC, Akers WJ, Sudlow G, Xu B, Laforest R and Achilefu S, Nanoscale, 2015, 7, 440–444. [PubMed: 25418982]
202. Pressly ED, Pierce RA, Connal LA, Hawker CJ and Liu Y, Bioconjug Chem, 2013, 24, 196–204. [PubMed: 23272904]
203. Nahrendorf M, Zhang H, Hembrador S, Panizzi P, Sosnovik DE, Aikawa E, Libby P, Swirski FK and Weissleder R, Circulation, 2008, 117, 379–387. [PubMed: 18158358]
204. Simone EA, Zern BJ, Chacko AM, Mikitsh JL, Blankemeyer ER, Muro S, Stan RV and Muzykantov VR, Biomaterials, 2012, 33, 5406–5413. [PubMed: 22560201]
205. Choi JH, Nguyen FT, Barone PW, Heller DA, Moll AE, Patel D, Boppart SA and Strano MS, Nano Lett, 2007, 7, 861–867. [PubMed: 17335265]
206. Ueno T, Dutta P, Keliher E, Leuschner F, Majmudar M, Marinelli B, Iwamoto Y, Figueiredo JL, Christen T, Swirski FK, Libby P, Weissleder R and Nahrendorf M, Circ Cardiovasc Imaging, 2013, 6, 568–573. [PubMed: 23771986]
207. Woodard PK, Liu Y, Pressly ED, Luehmann HP, Detering L, Sultan DE, Laforest R, McGrath AJ, Gropler RJ and Hawker CJ, Pharm Res, 2016, 33, 2400–2410. [PubMed: 27286872]
208. Chrastina A and Schnitzer JE, Int J Nanomedicine, 2010, 5, 653–659. [PubMed: 20856841]
209. Kim YH, Jeon J, Hong SH, Rhim WK, Lee YS, Youn H, Chung JK, Lee MC, Lee DS, Kang KW and Nam JM, Small, 2011, 7, 2052–2060. [PubMed: 21688390]
210. Tseng YC, Xu Z, Guley K, Yuan H and Huang L, Biomaterials, 2014, 35, 4688–4698. [PubMed: 24613050]
211. Cheng SH, Yu D, Tsai HM, Morshed RA, Kanojia D, Lo LW, Leoni L, Govind Y, Zhang L, Aboody KS, Lesniak MS, Chen CT and Balyasnikova IV, J Nucl Med, 2016, 57, 279–284. [PubMed: 26564318]
212. Zhao Y, Pang B, Luehmann H, Detering L, Yang X, Sultan D, Harpstrite S, Sharma V, Cutler CS, Xia Y and Liu Y, Adv Healthc Mater, 2016, 5, 928–935. [PubMed: 26865221]
213. Ahmad MW, Xu W, Kim SJ, Baeck JS, Chang Y, Bae JE, Chae KS, Park JA, Kim TJ and Lee GH, Sci Rep, 2015, 5, 8549. [PubMed: 25707374]
214. Zhou Z, Chen H, Lipowska M, Wang L, Yu Q, Yang X, Tiwari D, Yang L and Mao H, J Biomater Appl, 2013, 28, 100–111. [PubMed: 23812946]
215. Ma JJ, Yu MX, Zhang Z, Cai WG, Zhang ZL, Zhu HL, Cheng QY, Tian ZQ and Pang DW, Nanoscale, 2018, 10, 10699–10704.
216. Teraphongphom N, Chhour P, Eisenbrey JR, Naha PC, Witschey WR, Opasanont B, Jablonowski L, Cormode DP and Wheatley MA, Langmuir, 2015, 31, 11858–11867.
217. Liang M, Liu X, Cheng D, Liu G, Dou S, Wang Y, Rusckowski M and Hnatowich DJ, Bioconjug Chem, 2010, 21, 1385–1388. [PubMed: 20557066]
218. Fay F, Hansen L, Hectors S, Sanchez-Gaytan BL, Zhao Y, Tang J, Munitz J, Alaarg A, Braza MS, Gianella A, Aaronson SA, Reiner T, Kjems J, Langer R, Hoeben FJM, Janssen HM, Calcagno C, Strijkers GJ, Fayad ZA, Perez-Medina C and Mulder WJM, Bioconjug Chem, 2017, 28, 1413–1421. [PubMed: 28316241]
219. Yang C, Vu-Quang H, Husum DMU, Tingskov SJ, Vinding MS, Nielsen T, Song P, Nielsen NC, Norregaard R and Kjems J, Nanomedicine, 2017, 13, 2451–2462. [PubMed: 28842376]

220. Cui X, Mathe D, Kovacs N, Horvath I, Jauregui-Osoro M, Torres Martin de Rosales R, Mullen GE, Wong W, Yan Y, Kruger D, Khlobystov AN, Gimenez-Lopez M, Semjeni M, Szigeti K, Veres DS, Lu H, Hernandez I, Gillin WP, Protti A, Petik KK, Green MA and Blower PJ, Bioconjug Chem, 2016, 27, 319–328. [PubMed: 26172432]

221. Kircher MF, de la Zerda A, Jokerst JV, Zavaleta CL, Kempen PJ, Mittra E, Pitter K, Huang R, Campos C, Habte F, Sinclair R, Brennan CW, Mellinghoff IK, Holland EC and Gambhir SS, Nat Med, 2012, 18, 829–834. [PubMed: 22504484]

222. Kirschbaum K, Sonner JK, Zeller MW, Deumelandt K, Bode J, Sharma R, Kruwel T, Fischer M, Hoffmann A, Costa da Silva M, Muckenthaler MU, Wick W, Tews B, Chen JW, Heiland S, Bendszus M, Platten M and Breckwoldt MO, Proc Natl Acad Sci U S A, 2016, 113, 13227–13232.

223. Palekar RU, Jallouk AP, Lanza GM, Pan H and Wickline SA, Nanomedicine (Lond), 2015, 10, 1817–1832. [PubMed: 26080701]

224. Pan D, Kim B, Wang LV and Lanza GM, Wiley Interdiscip Rev Nanomed Nanobiotechnol, 2013, 5, 517–543. [PubMed: 23983210]

225. Zhang J, Yang C, Zhang R, Chen R, Zhang Z, Zhang W, Peng SH, Chen X, Liu G, Hsu CS and Lee CS, Adv Funct Mater, 2017, 27, DOI: 10.1002/adfm.201605094.

226. Lalwani G, Cai X, Nie L, Wang LV and Sitharaman B, Photoacoustics, 2013, 1, 62–67. [PubMed: 24490141]

227. Hong H, Gao T and Cai W, Nano Today, 2009, 4, 252–261. [PubMed: 21754949]

228. Zhang H, Wang T, Qiu W, Han Y, Sun Q, Zeng J, Yan F, Zheng H, Li Z and Gao M, Nano Lett, 2018, 18, 4985–4992. [PubMed: 29995426]

229. Lee H, Jang Y, Park S, Jang H, Park EJ, Kim HJ and Kim H, Theranostics, 2018, 8, 4247–4261. [PubMed: 30128051]

230. Yang F, Wang Q, Gu Z, Fang K, Marriott G and Gu N, ACS Appl Mater Interfaces, 2013, 5, 9217–9223. [PubMed: 23988030]

231. Tan X, Wang J, Pang X, Liu L, Sun Q, You Q, Tan F and Li N, ACS Appl Mater Interfaces, 2016, 8, 34991–35003.

232. Bao S, Huang S, Liu Y, Hu Y, Wang W, Ji M, Li H, Zhang NX, Song C and Duan S, Nanoscale, 2017, 9, 7284–7296. [PubMed: 28524912]

233. Kim S, Chen YS, Luke GP and Emelianov SY, Biomed Opt Express, 2011, 2, 2540–2550. [PubMed: 21991546]

234. Park JH, Dumani DS, Arsiwala A, Emelianov S and Kane RS, Nanoscale, 2018, 10, 15365–15370.

235. de la Zerda A, Liu Z, Bodapati S, Teed R, Vaithilingam S, Khuri-Yakub BT, Chen X, Dai H and Gambhir SS, Nano Lett, 2010, 10, 2168–2172. [PubMed: 20499887]

236. Li X, Wang D, Ran H, Hao L, Cao Y, Ao M, Zhang N, Song J, Zhang L, Yi H, Wang Z and Li P, Biochem Biophys Res Commun, 2018, 502, 255–261. [PubMed: 29802849]

237. Chen L, Ji Y, Hu X, Cui C, Liu H, Tang Y, Qi B, Niu Y, Hu X, Yu A and Fan Q, Nanoscale, 2018, 10, 13471–13484.

238. Donnelly EM, Kubelick KP, Dumani DS and Emelianov SY, Nano Lett, 2018, DOI: 10.1021/acs.nanolett.8b03305.

239. Ventola CL, P T, 2017, 42, 742–755. [PubMed: 29234213]

240. Bartneck M, Keul HA, Wambach M, Bornemann J, Gbureck U, Chatain N, Neuss S, Tacke F, Groll J and Zwadlo-Klarwasser G, Nanomedicine, 2012, 8, 1282–1292. [PubMed: 22406188]

241. Chen KH, Lundy DJ, Toh EK, Chen CH, Shih C, Chen P, Chang HC, Lai JJ, Stayton PS, Hoffman AS and Hsieh PC, Nanoscale, 2015, 7, 15863–15872.

242. Yu N, Wang Z, Zhang J, Liu Z, Zhu B, Yu J, Zhu M, Peng C and Chen Z, Biomaterials, 2018, 161, 279–291. [PubMed: 29425848]

243. Hallaj-Nezhadi S, Lotfipour F and Dass C, J Pharm Pharm Sci, 2010, 13, 472–485. [PubMed: 21092717]

244. Ma J, Xu R, Sun J, Zhao D, Tong J and Sun X, J Nanosci Nanotechnol, 2013, 13, 1472–1475. [PubMed: 23646663]

245. Tian T, Zhang T, Zhou T, Lin S, Shi S and Lin Y, Nanoscale, 2017, 9, 18402–18412.
246. Mao J, Tang S, Hong D, Zhao F, Niu M, Han X, Qi J, Bao H, Jiang Y, Fu C, Long D, Meng X and Su H, Nanoscale, 2017, 9, 3429–3439. [PubMed: 28233003]
247. Choi HS and Frangioni JV, Mol Imaging, 2010, 9, 291–310. [PubMed: 21084027]
248. Min Y, Caster JM, Eblan MJ and Wang AZ, Chem Rev, 2015, 115, 11147–11190.
249. Van Norman GA, JACC: Basic to Translational Science, 2016, 1, 170–179. [PubMed: 30167510]

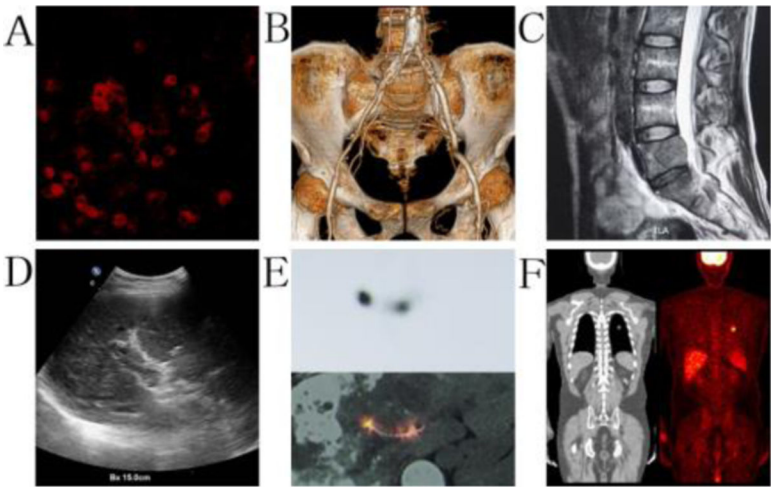

Fig. 1.

The primary imaging technologies in biomedical practice, including A: fluorescence image of tumor cells; B: CT diagnosis for artery stenosis; C: MRI image of lumber cancer metastasis; D: US detection of portal vein thrombosis; E: SPECT evaluation for ^{125}I seeds implantation; and F: PET detection of lung cancer tumor. All images were obtained from medical imaging research institute of China Medical University.

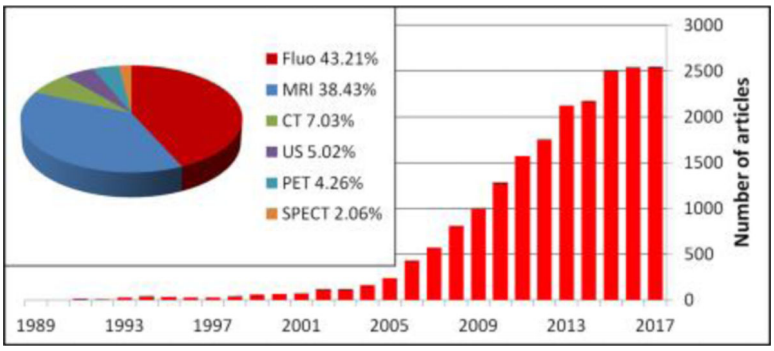

Fig. 2.

The number of publications searching for “nanoparticle and imaging” in Pubmed is rapidly increasing each year. Fluorescence and MRI imaging modalities represent the greatest areas of activity.

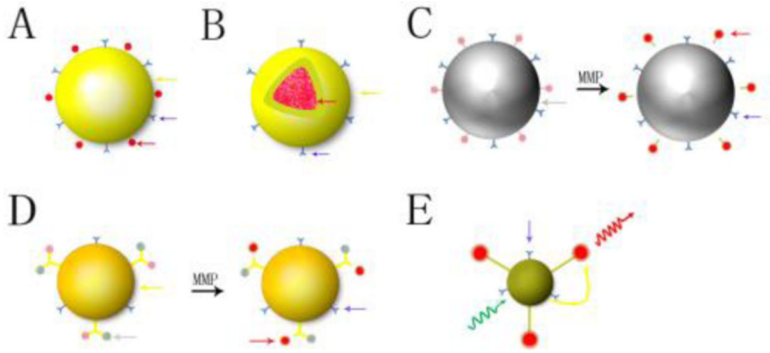

Fig. 3.

Different structure and composition of nanoparticles in fluorescence biomedical imaging. A: vector type; B: core-shell structure of NP; C: NP as a quencher; D: NP connected with fluorophore and quencher, E: Forster resonance energy transferred imaging NP (yellow arrow: nanoparticle; red arrow: fluorescent dye; blue arrow: ligand; grey arrow: quencher; yellow curve arrow: energy transfer; green curve arrow: excitation light; red curve arrow: emission light; MMP: matrix metalloproteinase).

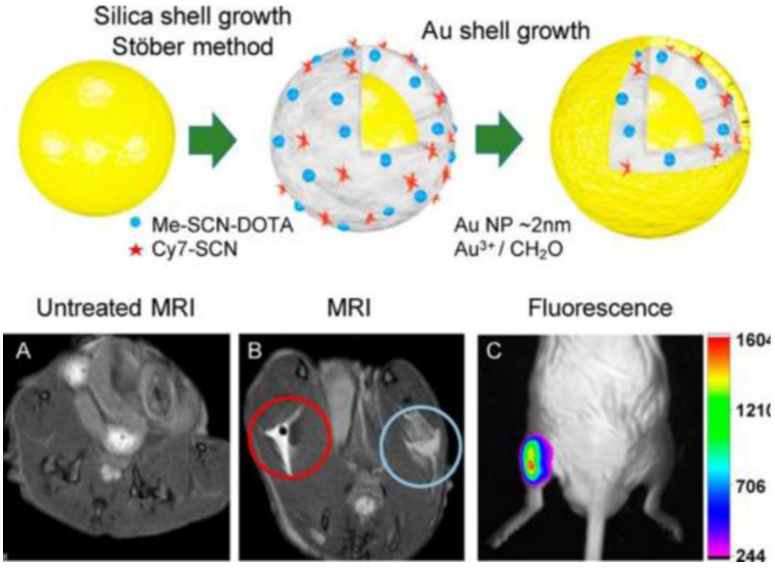

Fig. 4.

A safer T1 MRI contrast in a compact plasmonic nanoparticle with enhanced fluorescence was synthesized by a multilayer core-shell nanostructure, and known as nanomatryoshka (NM). Each NM consisted of an Au core, an Au shell and silica spacing layer encapsulated magnetic metal and fluorescent dye. This form protected fluorescent dye and reduced the metal release. Fe (III)-NM exhibited a 2× greater relaxivity than current MRI contrast agent (Gd-DOTA), and the photostability of fluorescent dye significantly increased (23×). Lower panel evaluated MRI and fluorescence imaging of FeCy7-NM in vivo. (A) Untreated in MRI, (B) Treated in MRI, red circle is nanoparticle and blue circle is saline, (C) Fluorescence imaging after injection. This nanoparticle can enable not only powerful tissue visualization with MRI but also fluorescence-based nanoparticle tracking. Reprinted with permission.[66] Copyright 2018. American Chemical Society.

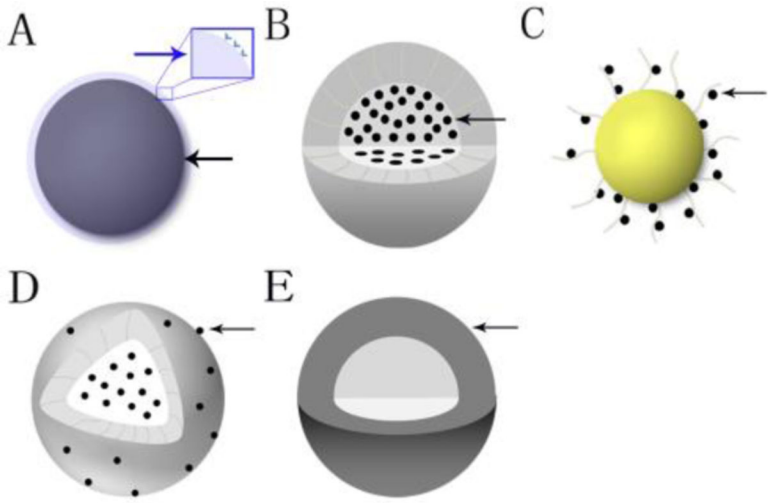

Fig. 5.

Different structures of MRI/CT imaging nanoparticles. A: basic structure; B core-shell structure; C: vector structure; D: mixed structure; E: core-shell structure. (Black arrow: MRI/CT imaging materials; Blue arrow: surface decoration.

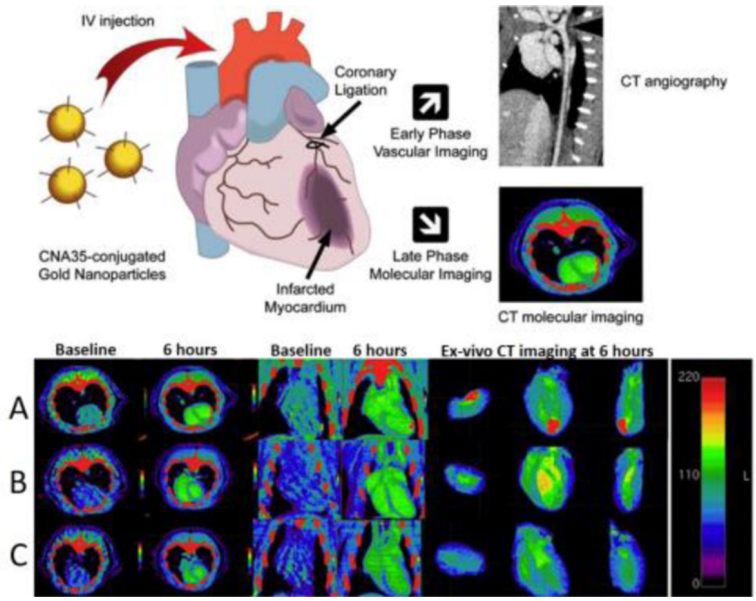

Fig. 6.

A CT-based molecular imaging nanoparticle was developed as blood pool and myocardial scar specific imaging contrast agent. Management of patients suffering from myocardial infarction is based on the extent of coronary artery stenosis and myocardial scar burden. (Upper panel) Gold nanoparticles (AuNPs) functionalized with collagen-binding adhesion protein 35 (CNA35) play the vascular imaging role at early phase and molecular imaging at late phase. (Lower panel) Animal experiment demonstrated a specific myocardial infaction imaging at 6 hours after injection (A). Control rat with myocardial infarction after injection of AuNPs (B) and rat without myocardial infaction after injection of CNA35-AuNPs (C) did not generate specific CT enhancement. This nanoparticle demonstrates a potential use for coronary artery imaging and myocardial infarction evaluation. Reproduced with permission.[173] Copyright 2018. Elsevier.

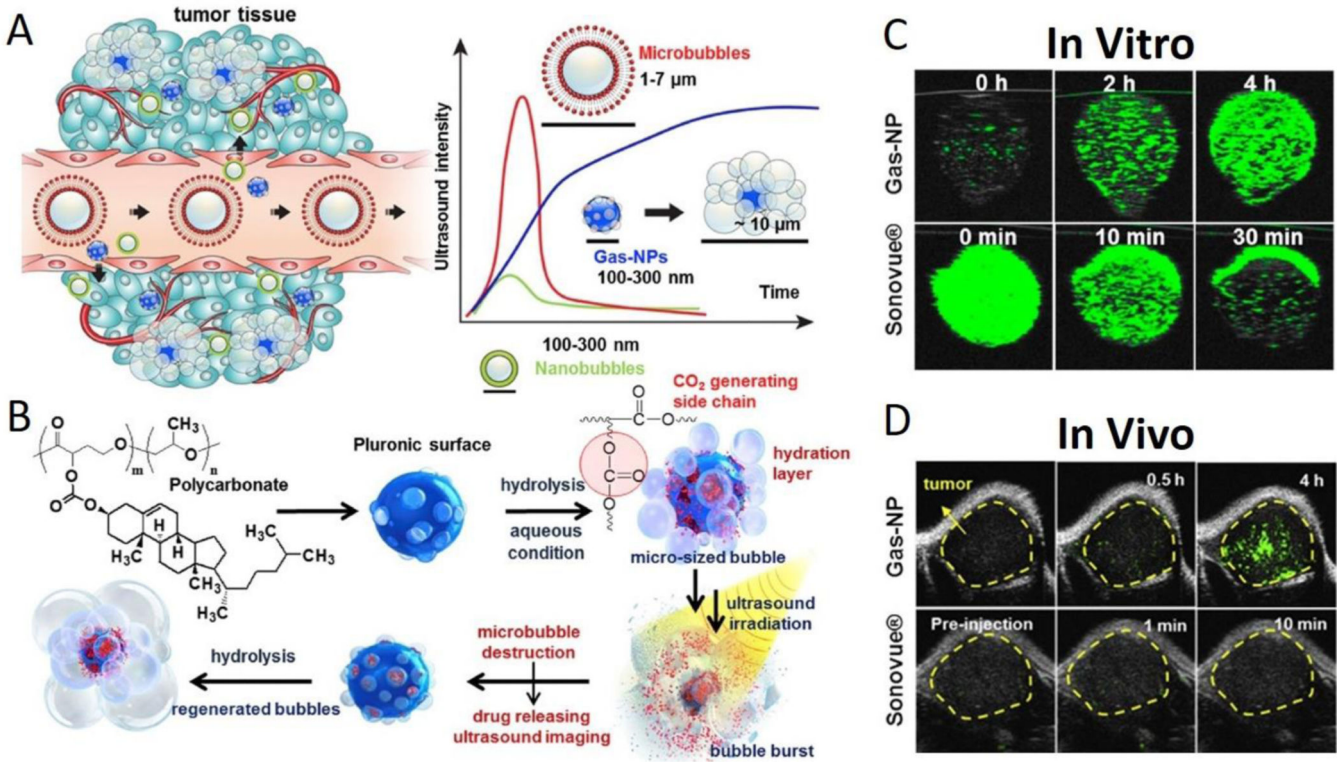

Fig. 7.

(A) Gas-NPs (blue nanoparticles) were synthesized via the O/W emulsion method with a size of 290nm and accumulated in tumor through the EPR effect. Current ultrasound contrast agents and large-sized perfluorocarbons-encapsulated microbubbles (red microparticles) present strong echo signals, but the large dimension prevents extravasation from vessel to surrounding tumor tissue. Also, small-sized nanobubbles (green nanoparticles) demonstrate a good biological distribution and effective extravasation, but the echo signals are not strong enough. (B) Chemical structure of hydrolysable carbonate copolymer; Poly(cholesteryl butyrolacone-co-propylene oxide). The carbonate copolymer was emulsified to produce solidified Gas-NPs via the O/W emulsion method. The Gas-NPs start to hydrolyze to produce CO2 nanobubbles in aqueous condition, followed by expansion/coalescence of nanobubbles into microbubbles for the targeted tumor US imaging. In addition, the anticancer drug-loaded Gas-NPs enable US-triggered drug delivery. (C) The US imaging test in vitro demonstrated a gradually CO2 generating process, current ultrasound contrast agent (Sonovue®) was the control (D) The ultrasound imaging ability in vivo showed a strong and persisted signals in whole tumor, current ultrasound contrast agent (Sonovue®) was the control. This nanoparticle demonstrates the unique and beneficial chemical gas-generating mechanism and is potentially useful for real-time ultrasound imaging and cancer therapy. Reproduced with permission.[190] Copyright 2016. Elsevier.

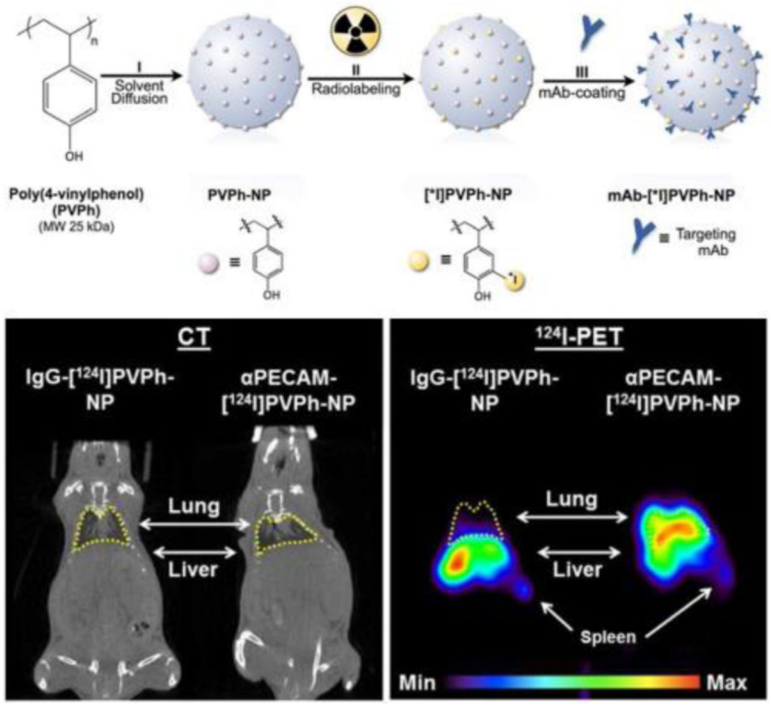

Fig. 8.

A PET imaging nanoparticle was synthesized from PVPh polymer and labeled with ^{124}I or ^{125}I, and then coated with specific targeting antibodies. Which endows a satisfactory endothelium PET imaging (lung). Reproduced with permission.[204] Copyright 2012. Elsevier.

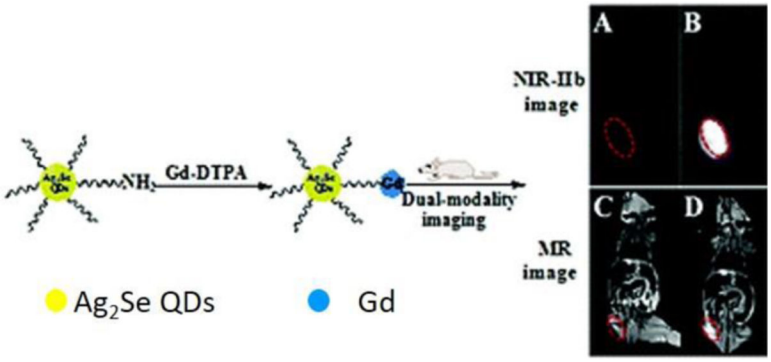

Fig. 9.

A dual-modality nanoparticle was developed with Ag_2Se quantum dots for fluorescence imaging and Gd-DTPA for MRI imaging. The excellent imaging efficiency indicate the potential value for multimodal imaging in clinical and scientific applications. Reproduced with permission.[215] Copyright 2018. Royal Society of Chemistry.

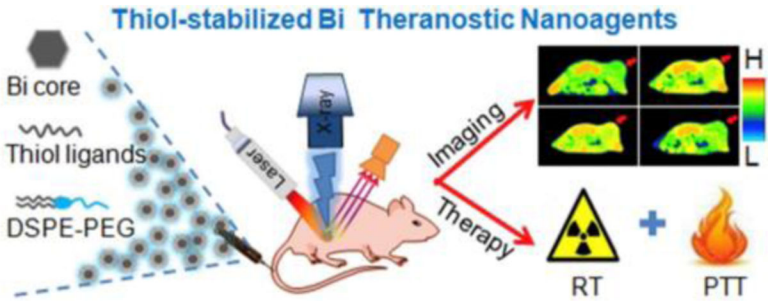

Fig. 10.

A theranostic nanoplatform was synthesized from thiol-capped Bi nanoparticles. They have a high X-ray attenuation coefficient and a strong photothermal conversion efficiency, which endow them with the simultaneous CT imaging, radiotherapy and thermotherapy. Reproduced with permission.[242] Copyright 2018. Elsevier.

Table 1

Selected examples of nanoparticles used in fluorescence biomedical applications

Author	NP type	Imaging agent	Size (nm)	Applications	Experimental model	Ref
Grebenik E,A	PMAO-(β-$NaY_{0.78}Yb_{0.2}Er_{0.02}F_4$)-Bs:Bn-scFc4D5	UCNP	120	Detecting early stage breast cancer	SK-BR-3 human cancer cells, CHO-K1 Chinese hamster ovary cells	61
Lee S	Cy5.5-substrate/AuNP	Cy5.5	20	Detecting protease activity	Mice bearing SCC7 tumors	67
Sun I,C	Cy5.5-DEVD-DOPAK/AuNP	Cy5.5	37.8	Testing caspase-3 to identify apoptosis activity in cells	HeLa cells	68
Chen L,J	PLNP($Zn_{1.1}Ga_{1.8}Ge_{0.1}O_4:Cr^{3+}$)-CuS-RGD	PLNP	141	Detecting tumor and guiding therapy	SCC-7 cells, 293T cells and athymic BALB/c nude mice bearing SCC-7 cells	69
Li L	DNAzymes(Zn-Enz)/AuNP-FAM/BHQ-1, DNAzymes(Cu-Enz)/AuNP-Cy5/BHQ-2	FAM,Cy5	13	Tracking ion of Zn and Cu in alive cell	HepG2 cells	70
Muthukumar T	CNP(Mtx-Asp-FITC)	FITC	90.9	Monitoring therapeutic drug delivery	A549 lung cancer cells	78
Markovic S	Cy7.5-INCeRT	Cy7.5	30, 200	Monitoring drug diffusion	Athymic nude mice	80
Zhao Y,M	QD710-Cy7-PEGylated lipids	Cy7	20	Monitoring NP accumulation and dissociation kinetics in tumor	Swiss nude mice bearing HCT-116 cells	85
Gao J,H	QD710-Dendron/RGD (InP/ZnS core/shell QDs)	Quantum dots	12	Targeted imaging tumor cells	BALB/c mice, athymic nude mice bearing SKOV3 tumors	87
Geng J,L	PFVBT(AuNP-PLGA)/(PLGA-PEG_{2000}-folate)	PFVBT	120	Detecting MCF-7 cell in breast cancer	Breast cancer cells (MCF-7)	94
Pu K,Y	Cationic oligofluorene substrated POSS	Ethidium bromide	3.6	Imaging double-stranded DNA	Breast cancer cells (MCF-7)	101
Blechinger J	Perylenediimide-containing polysiloxane core and silica shell	Perylenediimide	18, 70	Detecting nanotoxicity in alive cells	HeLa cells	102
Chen G,J	AB3-UCNP($NaYF_4$:Yb/Tm/Er)-RB/KE108	UCNP	14	Monitoring cellular uptake of nanoparticles and combined with therapy	TT cells (human thyroid cancer cells), athymic nude mice bearing TT cells	103
Iacono P	Au@IR-pHPMA	IR	55	Detecting lymph node	Nude mice	104

Nanoscale. Author manuscript; available in PMC 2021 May 11.

Table 2

Selected examples of nanoparticles used in MRI biomedical applications

Author	NP	size (nm)	Applications	Imaging	Experiment model	Ref
Winter P,M	Alpha(nu)beta(3)-Gd (paramagnetic particle)	273	Imaging angiogenesis	T1	VX-2 rabbit	50
Ghaghada K,B	Liposomal gadolinium	125	Imaging placenta as blood-pool contrast	T1	SD rats	113
Vargo K,B	Her2/neu-Oleosin-30G (Micelles)	74	Imaging target cells	T2	NIH/3T3 and T6–17 cells	114
Mekuria S,L	G4.5-Gd_2O_3-PEG	50.4	New T1/T2 MRI contrast agent	T1, T2	RAW264.7 cells, BALB/c mice	116
Zhang Z	SPIO	70–140	Tracking GFP gene marker	T2	GFP-R3230Ac cell line	123
Frias J,C	rHDL-Gd	14–17	Imaging and characterizing atherosclerotic plaques	T1	ApoE-/- mice	129
Rahmer J	RBC encapsulated iron particles	60	Blood-pool contrast with longer life-time	T1, T2	Mouse	130
Park I,K	USPIO-PEI	100	Determining nanoparticle vehicle unpackaging for gene	T2	HeLa cells	131
Mi P	PEGMnCaP NPs	60	PH-activatable contrast in cancer	T1, T2	Mice bearing C26 and HT-29 cells	132
Keca J,M	Mn-nanotexaphyrin	100	Imaging lymph node	T1, T2	BALB/c nude mice	133
Hu J	Micelles with PTX and SPIO	15–300	Delivering drug and MRI imaging	T2	Rabbit	134
Lanza G,M	TF-biotinylated perfluocarbon-(Gd-DTPA-BOA)@(doxorubicin /paclitaxel)	250	Evaluating and quantifying drug delivery system for vascular restenosis	T1	Porcine vascular smooth muscle cells	135
Starmans L,W	FibPep-ION-Micelles	40	Detecting and imaging thrombus	T2	Mouse	136
Jin A,Y	P-selectin-MNP(iron oxide)-PBP	50	Imaging post-stroke neuroinflammation	T2	C57BL/ 6 mice	137
Lu J	Mn-SPIO micella	80	High power liver imaging contrast	T2	In vivo	138
Oishi K	TMADM-03	44	Imaging pancreatic islet graft	T1, T2	BALB/c nude mice	139
Hachani R	DHCA functioned IONP labeled hMSCs	88.2	Imaging and tracking stem cells	T2	Swiss mice	140
Wang A,Z	TCL-SPION-Apt	66.4	Imaging prostate cancer cells and chemotherapy	T1, T2	LNCaP and PC3 cell line	141
Zhang C	HBPFPE-aptamer	7.8	Detecting breast cancer	^{19}F-MRI	Mice bearing MDA-MB-468 cells	142

Nanoscale. Author manuscript; available in PMC 2021 May 11.

Table 3

Select examples of nanoparticles used in CT scans

Author	NP	Size (nm)	Applications	Experiment model	Ref
Kim D	PSMA-specific aptamer conjugated AuNP	29.4	Imaging prostate cancer cells	LNCaP and PC3 prostate cancer cells	18
Bhavane R	Liposomal iodine	400	Imaging macrophage-rich atherosclerotic plaques	Apolipoprotein E-deficient mice	53
Ghaghada K,B	Liposomal-iodine	100	Identifying tumor vascular structure	Balb/c mice bearing 4T1/Luc cells	156
Bonitatibus P,J	Tantalum oxide	<6	Producing greater imaging capability than iodine	In vitro	157
Ahn S	AuNP	20	Incorporating RBC to image blood flow	In vitro	158
Chien C,C	AuNP	1	Labelling tumor cells to image tumor growth	Mice bearing EMT-6 and CT-26 cells	159
Hainfeld J,F	AuNP	11	Imaging brain malignant gliomas and enhancing radiotherapy	B6C3f1 mice bearing Tu-2449 cells	160
Silvestri A	AuNP	27–176	AuNP with CT contrast capability	Mice	161
Samei E	Liposomal iodine	113	Imaging tumor	Rat bearing R3230 AC cells	162
Betzer O	AuNP	20	Tracking mesenchymal stem cells	FSL rat	163

Table 4

Select examples of nanoparticles applied in ultrasound examinations

Author	NP	Size (nm)	Applications	Classification	Experiment model	Ref
Hu Y	FA-PEG-CS and perfluorooctyl bromide nanocore	229.5	Molecular tumor imaging agents	Liquid	Bel7402 and L02 cells	177
Seo M	Silica coated NP into perfluorobutane microbubble	Near 3000	Ultrasound imaging agents with potential therapeutic applications	Gas	In vitro	180
Wang C,W	C_3F_8-filled PLGA	152	Ultrasound imaging agents	Gas	Wister rat	184
Chen F	Exosome-like silica NP	30–150	Stem cell imaging agent	Solid	Label human mesenchymal stem cells and inject into nude mice	186
Zhang K	Rattle-type MSN	260	Ultrasound imaging agents	Solid	Rabbit vx2 tumor	187
Min H,S	Gas-NP	290	PH related contrast agents in tumor	Gas	C3H/HeN mice bearing SCC-7 cells	190
Liu J	PLA-herceptin	250	Specific detection of tumor molecular marker	Solid	SKBR-3 and MDA-MB-231 human breast cancer cells	191
Lee J	RVG-GNPs	220	PH related contrast agents in tumor	Gas	Athymic mice bearing N2a cells	192
Paproski R,J	Porphyrin nanodroplet	185	Tumor imaging contrast agent	Gas	Chicken embro HT1080-GFP and Hep3-GFP tumor	193
Peyman S,A	PFC-NP(C_4F_{10})	100–200	Ultrasound imaging agents	Gas	CD1 mice	194

Nanoscale. Author manuscript; available in PMC 2021 May 11.

Table 5

Select nanoparticles applied in PET/SPECT examinations

Author	NP	Size (nm)	Applications	Experiment model	Imaging modality	Ref
Lee S,B	^{18}F-labeled DBCO-PEGylated MSN	100–150	Imaging tumor	Mice bearing U87MG tumor	PET	196
Zern B,J	$^{125/124}$I-labeled anti-ICAM-1/PVPh-NP	200	Detecting pulmonary inflammation	Mice	PET	197
Schluep T	^{64}Cu labeled IT-101	37	Monitoring pharmacokinetics and tumor dynamics	Mice bearing neuro2A tumor	PET	198
Pressly E,D	^{64}Cu labeled CANF-comb nanoparticle	16–22	Imaging natriuretic peptide clearance receptor in prostate cancer	Athymic mice bearing CWR22 tumor cells	PET	202
Nahrendorf M	^{64}Cu-TNP	20	Imaging macrophages in inflammatory atherosclerosis	C57BL/6 mice deficient in apolipoprotein E	PET	203
Ueno T	^{64}Cu labeled CLIO-VT680	20	Detecting rejection and immunomodulation in cardiac allografts	C57BL/6 recipients of BALB/c allografts in mice	PET	206
Woodard P,K	^{64}Cu labeled CANF-comb nanoparticle	16–22	Imaging atherosclerosis in artery	C57BL/6 mice deficient in apolipoprotein E	PET	207
Chrastina A	^{125}I silver nanoparticle	12	Monitoring distribution of nanoparticles	BALB/C mice	SPECT	208
Kim Y,H	^{125}I labeled cRGD-PEG-AuNP	31	Detecting cancer cells and imaging tumor sites	U87MG, MCF7 cells and nude mice bearing U87MG cells	SPECT	209
Tseng Y,C	^{111}In labeled lipid/calcium/phosphate NPs	25	Imaging lymph node metastasis	C57BL/6 mice, nude mice and BALB/c mice bearing 4T1-Luc2-GFP cells	SPECT	210
Cheng S,H	^{111}In-MSN labeled neural stem cells	70	Tracking glioblastoma	Nude mice bearing U87MG cells	SPECT	211
Zhao Y	^{199}AuNPs(DAPTA)	5	Targeted imaging tumor	4T1 TNBC mouse	SPECT	212

Nanoscale. Author manuscript; available in PMC 2021 May 11.